CHAPTER 16 – REFERENCES

[1] Sheward, G.E., and Bell, G.R. "Development and evaluation of a Ni-Cr-P brazing filler metal". *Welding Journal*, vol. 55, no. 10. October 1976. pp. 285s-292s.

[2] *ASM Handbook: Volume 3 - Alloy Phase Diagrams*. ASM International, Metals Park, OH. 1992. pp. 2.127 (Ni-Cd binary phase diagram), 2.143 (Co-Hf binary phase diagram), 2.241 (Ni-Hf binary phase diagram), 2.321 (Ni-Zn binary phase diagram) and 2.322 (Ni-Zr binary phase diagram).

[3] Lugscheider, E., and Kim D.-S. "New low-melting nickel-based high-temperature brazing alloys". *Schweissen und Schneiden*, vol. 43, no. 4. April 1991. pp. 222-226.

[4] Lugscheider, E., and Partz, K.-D. "High-temperature brazing of stainless steel with nickel-base filler metals BNi-2, BNi-5 and BNi-7". *Welding Journal*, vol. 62, no. 6. June 1983. pp. 160s-165s.

[5] Johnson, C. "The use of TETIG diagrams in high-temperature brazing". *Welding Journal*, vol. 60, no. 10. October 1981. pp. 185s-193s.

[6] Sakamoto, A., Fujiwara, C., Hattori, T, and Sakai, S. "Optimizing processing variables in high-temperature brazing with nickel-based filler metals". *Welding Journal*, vol. 68, no. 3. March 1989. pp. 63-71.

[7] Miyazawa, Y., and Ariga, T. "A study of the brazeability of nickel-based brazing filler metal foil for joining nickel base metal to mild steel base metal". *Welding Journal*, vol. 71, no. 7. July 1993. pp. 294s-300s.

[8] Kavishe, F.P.L., and Baker, T.J. "Influence of joint gap width on strength and fracture toughness of copper brazed steels". *Materials Science and Technology*, vol. 6, no. 2. February 1990. pp. 176-181.

[9] Lugscheider, E., and Krappitz, H. "The influence of brazing conditions on the impact strength of high-temperature brazed joints". *Welding Journal*, vol. 65, no. 10. October 1986. pp. 261s-267s.

[10] Draugelates, U., and Hartmann, K.-H. "Behaviour of brazed nickel alloy under cyclic and thermal load". *Welding Journal*, vol. 57, no. 10. October 1978. pp. 298s-302s.

[11] Tung, S.K., Lim, L.C., and Lai, M.O. "Solidification phenomena in nickel base brazes containing boron and silicon". *Scripta Materialia*, vol. 34, no. 5. March 1996. pp. 763-769.

[12] Johnson, R. "Microstructural aspects of brazing a ferritic steel with two Ni-Si-B braze filler metals". *Welding Journal*, vol. 57, no. 4. April 1978. pp. 93s-102s.

[13] Gale, W.F., and Wallach, E.R. "Influence of isothermal solidification on microstructural development in Ni-Si-B filler metals". *Materials Science and Technology*, vol. 7, no. 12. December 1991. pp. 1143-1148.

[14] Lasalmonie, A. "Diffusion brazing of nickel based superalloys: some basic aspects". *Annales de Chimie France*, vol. 12, no. 3. 1987. pp. 247-257.

[15] Savage, E.I., and Kane, J.J. "Microstructural characterisation of nickel braze joints as a function of thermal exposure". *Welding Journal*, vol. 63, no. 10. October 1984. pp. 316s-323s.

[16] Tung, S.K., Lim, L.C., and Lai, M.O. "Microstructural evolution and control in BNi-4 brazed joints of nickel 270". *Scripta Metallurgica et Materialia*, vol. 33, no. 8. October 1995. pp. 1253-1259.

[17] Lecomte-Martens. *Private communication* (repair company C.R.M., Belgium).

[18] Elder, J.E., Thamburaj, R., and Patnaik, P.C. "Braze repair of MA754 aero gas turbine engine nozzles". Proceedings of the *ASME Gas Turbine and Aeroengine Congress and Exposition* (Paper No. 89-GT-235). 4-8 June 1989. Toronto, Canada.

[19] Rose, D.P., Price, G., and Thyssen, J. "Development and evaluation of a repair for saddle cracks in a radial flow turbine wheel". Proceedings of the *Conference on Life Assessment & Repair: Technology for Combustion Turbine Hot Section Components*. 17-19 April 1990. Phoenix, Arizona, United States of America. pp. 271-286.

[20] Lee, J.W., McMurray, H.J., and Miller, J.A. "Development of a new brazing technique for repair of turbine engine components". *Welding Journal*, vol. 64, no. 10. October 1985. pp. 18-21.

[21] Hoppin, G.S., and Berry, T.F. "Activated Diffusion Bonding". *Welding Journal*, vol. 49, no. 11. November 1970. pp. 505s-509s.

[22] Demo, W.A., and Ferrigno, S.J. "Brazing method helps repair aircraft gas-turbine nozzles". *Advanced Materials & Processes*, vol. 131, no. 3. March 1992. pp. 43-45.

[23] Young, W.R. "Turbine airfoil repair". Proceedings of the *Conference on Materials Synergisms*. October 1978. Kiamesha Lake, New York, United States of America. pp. 924-938.

[24] Knotek, O., and Lugscheider, E. "Brazing filler metals based on reacting Ni-Cr-B-Si alloys". *Welding Journal*, vol. 55, no. 10. October 1976. pp. 314s-318s.

[25] Van Esch, H. "Braze repair techniques for gas turbine blades and vanes". *Turbomachinery International*, vol. 27, no. 7. September 1986. pp. 29-32.

[26] Su, C.Y., Chou, C.P., Wu, B.C., and Lih, W.C. "Microstructural characterisation of transient liquid phase zone of activated diffusion brazed nickel base superalloy". *Materials Science and Technology*, vol. 15, no. 3. March 1999. pp. 316-322.

[27] Chasteen, J.W., and Metzger, G.E. "Brazing of Hastelloy X with wide clearance butt joints". *Welding Journal*, vol. 58, no. 4. April 1979. pp. 111s-117s.

[28] Liburdi, J., Lowden, P., and Ellison, K. "Powder metallurgy repair technique." *US patent number US5156321*. 27 August 1990 (application date).

[29] Jahnke, B., and Demny, J. "Microstructural investigations of nickel-based repair coating processed by liquid phase diffusion sintering". *Thin Solid Films*, vol. 110, no. 3. December 1983. pp. 225-235.

[30] Miglietti, W.M., Curtis, R., Hall, B., and Lazarin, C.M. "Liquid phase diffusion bond repair of Westinghaus 501F, row 3 vanes". Proceedings of the *ASME Turbo Expo Conference 2000*. 2000. Münich, Germany.

[31] Miglietti, W.M., Kearney, J., and Pabon, L. "Liquid phase diffusion bond repair of Siemens V84.2, row 2 vanes and Alstom Tornado 2nd stage stator segments". Proceedings of the *ASME Turbo Expo Conference 2001*. 2001. New Orleans, United States of America.

[32] Miglietti, W.M.A. "Wide gap diffusion braze repair of Co-based industrial turbine vanes". Proceedings of the *International Brazing & Soldering Conference*. 2-5 April 2000. Albuquerque, New Mexico, United States of America. pp. 476-485.

[33] Miglietti, W.M.A. "Wide gap diffusion braze repair of Ni-based industrial turbine vanes". Proceedings of the *6th International Conference on Brazing, High Temperature Brazing and Diffusion Welding*. DVS Berichte, no. 212. 8-10 May 2001. Aachen, Germany. pp. 107-112.

APPENDIX A

MIGLIETTI, W.M., CURTIS, R., HALL, B., AND LAZARIN, C.M. "LIQUID PHASE DIFFUSION BOND REPAIR OF WESTINGHAUS 501F, ROW 3 VANES". PROCEEDINGS OF THE *ASME TURBO EXPO CONFERENCE 2000*. 2000. MÜNICH, GERMANY.

LIQUID PHASE DIFFUSION BOND REPAIR OF WESTINGHOUSE 501F, ROW 3 VANES

Warren M Miglietti , Rich Curtis, Brandon Hall and Christina M Lazarin
Sermatech International, Inc., Manchester, CT, 06040

ABSTRACT

During the industrial turbine engine operation of the W501F, Row3 Vanes, cracks develop as a result of thermal fatigue. Other damage found is pitting and dents resulting from corrosion/oxidation and FOD (foreign object damage) respectively. Erosion damage is also commonly found on the airfoils. Finally there is downstream deflection of the inner buttress/seal areas, as a result of axial creep. This paper describes the vacuum LPDB (liquid phase diffusion bond) repair process used to repair all of the above-mentioned damage, including LPDB build up and machining of the hook fit areas.

As a means of qualifying the high temperature diffusion bond process, both metallurgical and mechanical property evaluations were carried out. The metallurgical evaluation consisted of optical and scanning electron microscopy. The wide gap diffusion bonded area consisted of a fine-grained structure with carbide and boride phases dispersed both intergranularly and intragranularly. An EDAX analysis was also conducted and the results are reported.

The chemistry of the repaired area is similar to the base metal which may explain why mechanical tests revealed properties equivalent to that of the base metal. The mechanical evaluations undertaken were tensile tests at room temperature and elevated temperature, as well as stress rupture tests. These results were equivalent to mechanical properties of the X-45 Co-based superalloy, which is the base metal of the vane.

INTRODUCTION

Brazing has been utilised for decades now to repair aircraft engine vane and nozzle segments. It has only being the last 5 years that a variant of brazing has been utilised for Industrial Gas Turbine (IGT) vane and nozzle repairs. The wide gap brazing process was made popular by GE's and Pratt and Whitney's ADH (activated diffusion healing) (Demo and Ferrigno,1992) and Turbofix processes respectively. Many repair vendors have their own proprietary wide gap braze process such as SNECMA's RBD (rechargement per brasage diffusion), Howmet's ESR (effective structural repair) (Wustman and Smith,1996), and Chromalloy's SRB (surface reaction braze) (Bell,1985). Other wide gap joining processes available are LPDS (liquid phase diffusion sintering), Liburdi's LPM (Liburdi powder metallurgy) (Ellison, Lowden and Liburdi,1992) and Sermatech's "Sermafill" process. The latter 3 processes do not comply exactly with the definition of brazing as defined by the American Welding Society (AWS Welding Handbook, Vol. 2). Hence liquid phase diffusion sintering as referred to by Siemens/Westinghouse, powder metallurgy as referred to by Liburdi Engineering and liquid phase diffusion bonding (LPDB) as referred to by Sermatech are relatively new names appearing on the technological list of techniques to repair vanes and nozzles.

The object of this paper is to describe the use of the liquid phase diffusion bonding process, (which Sermatech have as their trademark the Sermafill process) for Westinghouse 501F, Row 3 vane repairs, and to compare this process with the traditional wide gap braze process. The former process is proprietary and hence exact precise temperatures and times, chemical compositions etc. cannot be documented; nevertheless, ranges of temperature and times are documented.

The LPDB process was qualified by undertaking a metallurgical evaluation and a mechanical property evaluation to show that metallurgically sound and high strength joints resulted. This LPDB process was used to restore wall thickness on the concave and convex surfaces of the airfoil, repair cracks,

pits/dents and build up the hook fit areas as a result of downstream deflection of the inner buttress/seal areas, as a result of axial creep. Figure 1 shows a typical example of a W501F, Row 3 vane with 3 airfoils. The vane is cast from a Cobalt superalloy referred to as X-45. Its chemical composition is Co-25.5Cr-10.5Ni-7W-0.25C-2(max)Fe-0.010B. The high Cr content contributes to corrosion, low temperature oxidation and sulphidation resistance.

Figure 2 shows typical cracking on the shroud and fillet areas as revealed by FPI (fluorescent particle inspection), while fig's 3, 4 and 5 show individual cracks in more detail. These cracks are wide 2.5mm (0.1'') and hence conventional narrow gap brazing cannot be utilised as a repair technique. The hook fit area, which needs to be rebuilt, is shown in fig 6.

Figure 1 – View of W501F, Row 3 vane

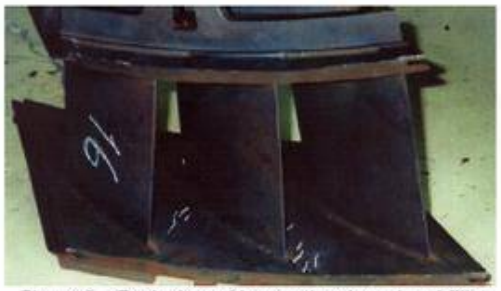

Figure 2 – Typical cracking on the shroud and fillet areas

The largest width of crack found on this engine set was 3.2mm (0.125''). Therefore for the process qualification the mechanical property tests (namely tensile and stress rupture) where undertaken on samples where the joint gap was 3.2mm (0.125''). The process is not limited to this gap and the largest gap repaired to date has been 10mm.

PROCESS EXPERIMENTAL PROCEDURE

Tensile tests at room temperature (21°C) and elevated

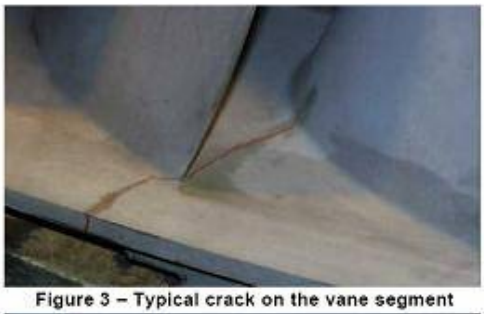

Figure 3 – Typical crack on the vane segment

Figure 4 – Typical crack on the vane segment

Figure 5 – Typical crack on the vane segment

Figure 6 – Hook fit area, which needs to be restored

temperatures, as well as stress rupture tests were undertaken. The test specimens were prepared in a butt joint configuration as seen in fig 7. The joint is in the centre of the gauge length and was 3.2mm wide.

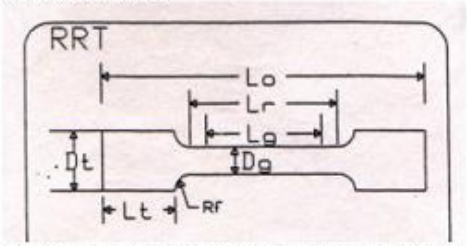

D_g=4.57mm, L_g=18.29mm, L_r=21.84mm, L_o=46.51mm, R_f =3.18mm, D_t=(5/16-24NF-2A inches) and L_t=9.53mm

Figure 7 – Configuration of tensile and stress rupture test specimens

Figure 8 shows the set up for the samples utilised for the metallographic evaluation. Molybdenum sheet stock was utilised to keep the joint gap uniform at 3.2mm in width. Conventional metallographic techniques were used for the metallurgical investigation.

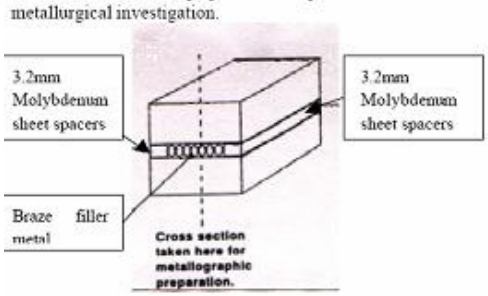

Figure 8 – Schematic representation of sample set for metallurgical evaluation

TENSILE AND STRESS RUPTURE TEST SPECIMEN PREPARATION

Mechanical test specimens according to the configuration shown in fig 7 were prepared as follows:

a) Obtain scrap vane and cut/grind away sections from the shroud area of the vane.
b) Machine rectangular sections of 12.5mm (0.5'') X 12.5mm (0.5'') X 55.9mm (2.2'')
c) Cut sample in half.
d) Grind the mating surfaces flat.
e) Grit blast surfaces with silicon carbide.
f) Shim gap at 3.2mm (0.125'').
g) Apply paste to the joint gap.
h) Place samples in fixture to maintain alignment.
i) Set in vacuum furnace.
j) Process between 1120°C (2048°F) and 1200°C (2192°F).
k) Isothermally process at the above-mentioned range for 4-20 hours.
l) Age at 982°C (1800°F) for 4hours.
m) Machine samples to the configuration shown in fig 7.
n) Send machined specimens for X-ray to determine if porosity greater than 1.3mm (0.050'') and for lack of bonding to the mating surfaces exist.

RESULTS AND DISCUSSION OF MECHANICAL PROPERTY TESTING

Table 1 below shows the results of the tensile tests undertaken at room temperature and elevated temperatures of 650°C, 760°C and 980°C. As can be seen the tensile and yield strengths are equivalent to the values quoted in the Metals Handbook. The ductility of the "Sermafill" joints appears low, and is typically 25-51% of the values quoted in the Metals Handbook.

Table 1: Tensile Strength of X-45 processed with "Sermafill"1 Filler Metal

TEMPERATURE		TENSILE STRENGTH		YIELD STRENGTH		ELONGATION	RA
°C	°F	MPa	ksi	MPa	Ksi	%	%
21	70	773	112	505	73.2	4.5	1.6
21	70	763	110	531	77	4.4	1.6
21	**70**	**745**	**108**	**525**	**76**	**8**	?
650	1200	520	75.4	304	46.8	6.4	7.1
650	1200	446	64.6	306	44.3	3.1	4.3
650	**1200**	**515**	**74.6**	**260**	**38**	**12**	?
760	1400	509	73.8	311	45.1	2.9	3.9
760	1400	451	65.4	315	45.7	3.6	3.6
760	1400	450	65.2	341	49.4	2.9	3.9
760	1400	448	64.9	311	45.1	3.3	3.1
760	**1400**	**485**	**70**	?	?	**9**	?
980	1800	214	31	?	?	4.9	?
980	**1800**	**200**	**29**	?	?	**16**	?

NOTE: **Values in Bold are for X-45 parent alloy (Metals Handbook Vol3, ninth edition)**

To verify if the elongation is as low as the data indicates, some X-45 material was taken from the shroud area of a vane. This material was machined to the configuration shown in fig 7 and subjected to the Sermafill heat treatment cycle. Table 2 shows the results of the X-45 specimens removed from the vane segment.

As seen in Table 2 the mechanical properties of the X-45 taken from the actual vane casting is lower than that quoted in the Metals Handbook, especially the ductility. Therefore the Sermafill joints have ductility in the order of 80% of the X-45 casting material. This is acceptable and the 20% loss in ductility

is attributed to the few brittle boride phases present in the 3.2mm (0.125") wide gap joint.

Table 2: Tensile strength of X-45 material taken from the vane

TEMPERATURE		TENSILE STRENGTH		YIELD STRENGTH		ELONGATION	RA
°C	°F	MPa	ksi	MPa	ksi	%	%
21	70	738	107	514	74.5	5.6	5.6
21	**70**	**745**	**108**	**525**	**76**	**8**	**?**

NOTE: **Values in Bold are for X-45 parent alloy (Metals Handbook Vol3, ninth edition)**

Table 3 shows the stress rupture properties of the "Sermafill 1" joints

Table 3: Stress rupture properties of X-45 processed with " Sermafill" 1 Filler Metal

TEMPERATURE		STRESS LEVEL		HOURS TO FAILURE	ELONGATION	RA
°C	°F	MPa	ksi	hrs	%	%
760	1400	260	38	92	?	?
760	**1400**	**260**	**38**	**100**	**?**	**?**
760	1400	193.2	28	513.9*	31.7	48.3
760	1400	193.2	28	566.5*	29.1	48.1
760	1400	193.2	28	507.1*	35.2	48.5
871	1600	103.5	15	365*	27.7	34.5
871	1600	103.5	15	344.2*	16.4	33.6
871	1600	103.5	15	336.3*	20.7	32

NOTE: **Values in Bold are for X-45 alloy (Metals Handbook Vol3, ninth edition)**

- **means that failure occurred in the base metal**

As seen in Table 3, the stress rupture properties of the joints are a minimum of 92% of the base metals stress rupture properties. In fact most of the failure occurred in the base metal, which is a good result.

To compare the results of the Sermafill wide gap joints with a more tradtional wide gap braze process, a 70%X-45 and 30%braze mixture was developed. Some samples were brazed with the same joint gap and at the same process parameters as those of the "Sermafill" joints. The 30% braze used in the mixture had a composition Co-40Ni-24.5Cr-3B.

Tables 4 and 5 show the tensile test results and stress rupture results respectively, of the joints brazed with the 70/30 mixture. As seen in these tables the strength of the brazed joint is 74%-80% of the base metals strength, the elongation is 50% of the cast X-45 vane material and the stress rupture life varies from 58-62% of the parent metals life. This is undesirable if the objective is to have a structural repair, where the properties of the repaired areas are equivalent to the base metal. Clearly the "Sermafill" type joints have superior mechanical properties when compared to a more traditional wide gap braze joint, and the properties are equivalent to the base metal as seen in Tables 1 and 3.

Table 4: Tensile strength of X-45 brazed with a traditional type filler metal

TEMPERATURE		TENSILE STRENGTH		YIELD STRENGTH		ELONGATION	RA
°C	°F	MPa	ksi	MPa	ksi	%	%
21	70	555.5	80.5	466.4	67.6	2.6	3.3
21	70	554.1	80.3	437.5	63.4	2.8	2.4
21	70	531.3	77.0	444.7	64.3	3.4	4.8
21	**70**	**745**	**108**	**525**	**76**	**9**	**?**
21	70	738	107	514	74.5	5.6	5.6
540	1004	405	58.7	254.6	36.9	3.1	2.6
540	1004	411.9	59.7	253.9	36.8	3.5	2.2
540	1004	380.9	55.2	285	41.3	4.9	1.9
540	1004	391	56.7	300.3	43.5	2.1	1.7
540	**1004**	**550**	**79.7**	**275**	**40**	**17**	**?**
650	1200	381.6	55.3	216.7	31.4	6.3	3.1
650	1200	391.2	56.7	216.7	31.4	3.4	1.7
650	1200	400.2	58	228.4	33.1	3.7	2.3
650	1200	393.3	57	227.7	33	3.6	2.2
650	**1200**	**515**	**74.6**	**260**	**38**	**12**	**?**

NOTE: **Values In Bold Are For X-45 Alloy (Metals Handbook Vol3, ninth edition)**

NOTE: Values underlined are from an actual cast vane

Table 5: Stress Rupture properties of X-45 brazed with a traditional type filler metal

TEMPERATURE		STRESS LEVEL		HOURS TO FAILURE	ELONGATION	RA
°C	°F	MPa	ksi	hrs	%	%
760	1400	260	38	61.4	?	?
760	1400	260	38	58.2	?	?
760	**1400**	**193.2**	**38**	**100**	**?**	**?**

NOTE: **Values in Bold are for X-45 alloy (Metals Handbook Vol3, ninth edition)**

RESULTS AND DISCUSSION OF THE METALLURGICAL EVALUATION

Figure 9 shows the microstructure of the base metal, which consists of a dendritic structure with Cr-carbides occurring intergranularly.

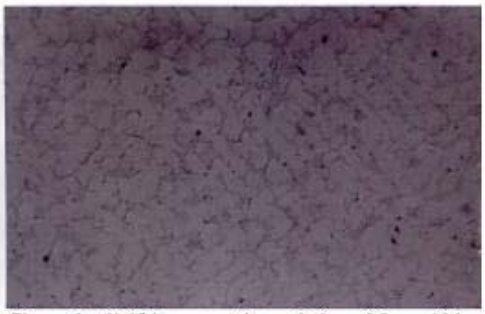

Figure 9 – X-45 base metal consisting of Cr-carbides dispersed intergranularly. Mag. 50X

Figures 10, 11, 12 and 13 all show the "Sermafill'ed" joint on the X-45 substrate, at increasing levels of magnification. Some boride phases can be seen in fig 13 and they resemble the Cr-carbide phases present in the base metal.

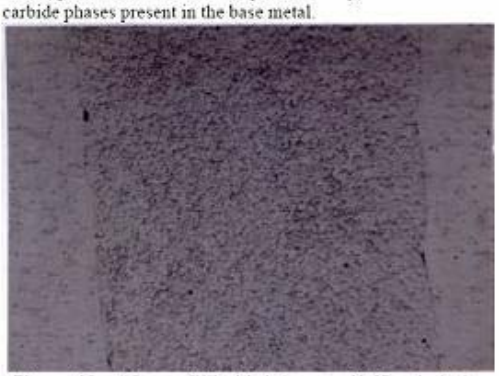

Figure 10 – "Sermafill'ed joint on an X-45 substrate. Mag. 50X

Figure 11 – LPD Bonded "Sermafill'ed joint on a X-45 substrate. Mag.100X

Figure 14 shows the joint interface. Clearly there is excellent bonding and adhesion to the mating surfaces.

A stress rupture sample (#3), which was tested at 760°C/193.2MPa and failed in the base metal, was subjected to a metallurgical evaluation using optical and scanning electron microscopy. Figure 15 shows the fractured piece, where the joint is intact. A semi quantitative and qualitative analyses on the base metal and joint can be seen in fig's 16 and 17. Essentially the elements of Co, Cr, Ni and W were found in the X-45 base metal, except the W concentration was higher than normal. (Perhaps the analysis was taken close to a W-carbide phase.) The LPD bonded joint had the same elements as the base metal, except for Ta, which is present in the chemistry of the "Sermafill" paste.

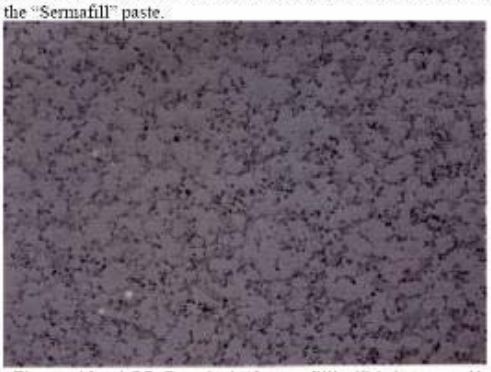

Figure 12 – LPD Bonded "Sermafill'ed" joint on a X-45 substrate. Mag. 200X

Figure 13 – LPD Bonded "Sermafill'ed" joint on a X-45 substrate. Mag. 500X

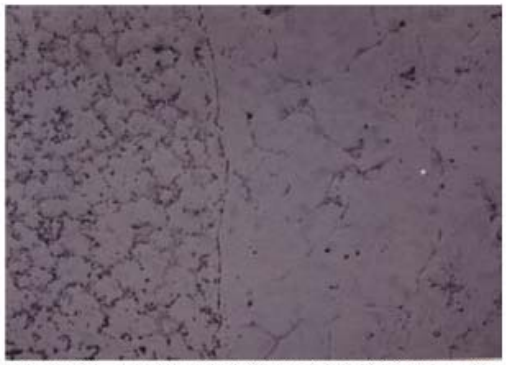

Figure 14 – LPD Bonded "Sermafill'ed" joint on a X-45 substrate. Mag. 200X

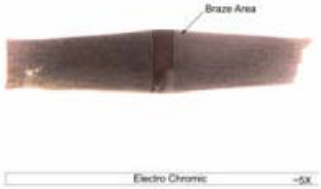

Figure 15 – Fractured stress rupture sample

Figure 16 – Semi-qualitative and semi-quantitative analylsis of the X-45 base metal

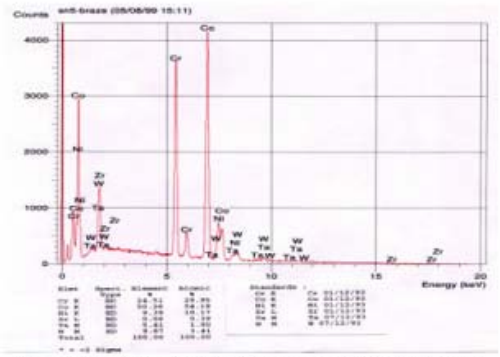

Figure 17 – Semi-qualitative and semi-quantitative analysis of the LPD bonded joint

Figures 18, 19, 20 and 21 show the above-mentioned stress ruptured LPD bonded joint at increasing magnifications. The phases seen on the grain boundaries in figure 22, are either Cr-borides or carbides, and W-borides or carbides respectively, as represented in the semi-qualitative and quantitative analyses seen in figures 23 and 24. As the EDAX system on the SEM could not detect either B or C it was difficult to precisely state the phases that formed in the joint.

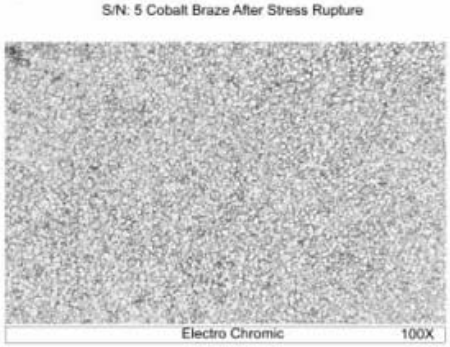

Figure 18 – Microstructure of a stress rupture tested, LPD bonded joint on a X-45 substrate. Mag. 100X

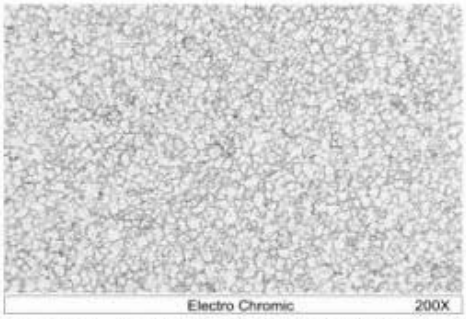

Figure 19 – Microstructure of a stress rupture tested, LPD Bonded joint on a X-45 substrate. Mag. 200X

S/N: 5 Cobalt Braze After Stress Rupture

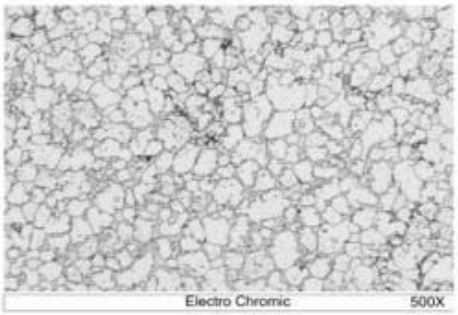

Figure 20 – Microstructure of a stress rupture tested, LPD Bonded joint on a X-45 substrate. Mag. 500X

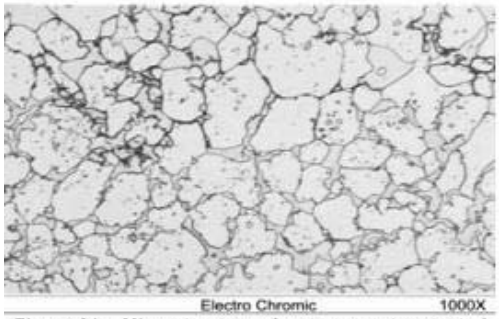

Figure 21 – Microstructure of a stress rupture tested, LPD Bonded joint on a X-45 substrate. Mag. 1000X

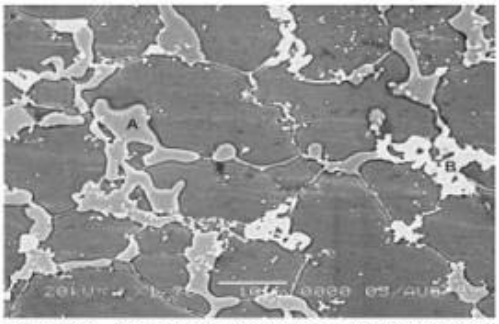

Figure 22 – Phases analysed on the grain boundaries of the LPD bonded joints.

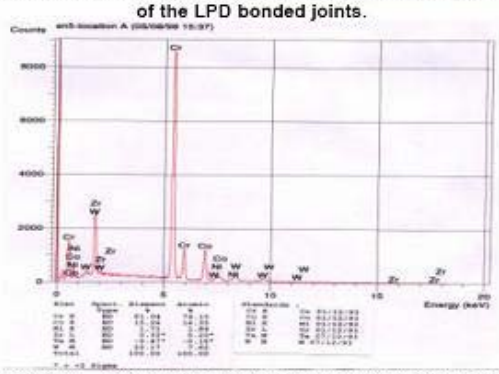

Figure 23 – Semi-qualitative and semi-quantitative analysis of the phase labeled "A" along the grain boundaries of a LPD bonded joint, after stress rupture testing.

The samples which, where wide gap brazed and the tensile and stress rupture test results were reported in Tables 4 and 5 respectively, were also metallographically examined to find a reason for the reduction in mechanical properties when compared to the LPD bonded joints. Figure 25 shows a macrograph of the brazed area. Figures 26, 27, 28 and 29 all show the wide gap braze joint at different magnifications. Clearly as seen in fig's 28 and 29, the grain boundaries of the joint consist of a large network/chain of elongated brittle boride phases. Comparing fig's 20 and 21, with 28 and 29, there is clear distinguishable difference as to the grain boundary morphology of the LPD bonded joints and the wide gap braze joints. The large network/chain of elongated brittle boride phases in the wide gap brazed joint is the predominant reason for the reduction in mechanical properties, including elongation.

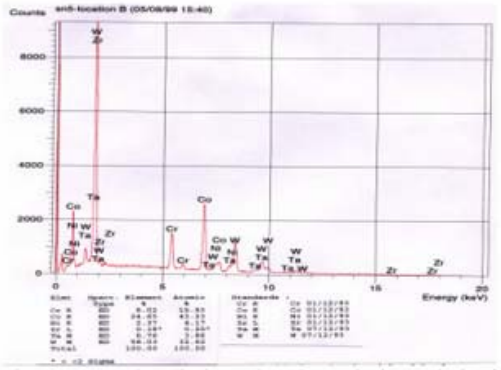

Figure 24 – Semi-qualitative and semi-quantitative analysis of the phase labeled "B" along the grain boundaries of a LPD bonded joint, after stress rupture testing.

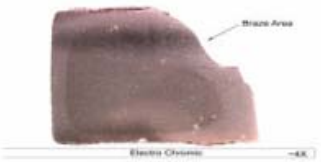

Figure 25 – Macrograph of the wide gap brazed joint.

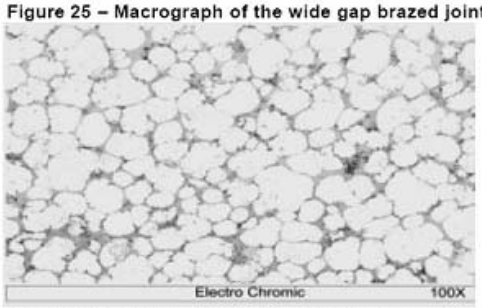

Figure 26 – Traditional type wide gap brazed joint on a X-45 substrate. Mag.100X

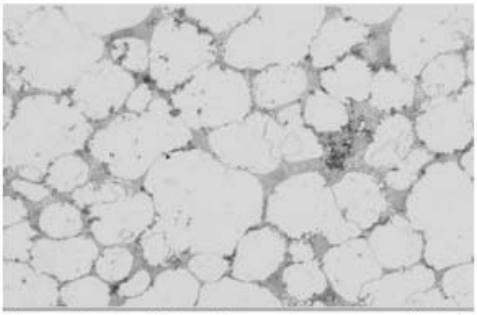

Figure 27 – Traditional type wide gap brazed joint on a X-45 substrate. Mag. 200X

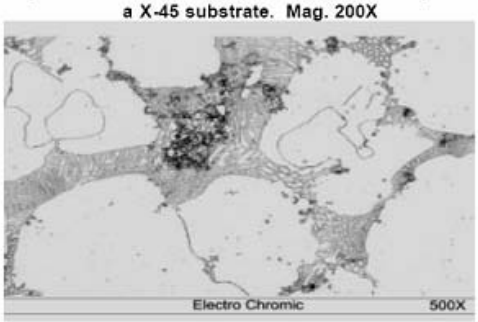

Figure 28 – Traditional type wide gap brazed joint on a X-45 substrate. Mag. 500X

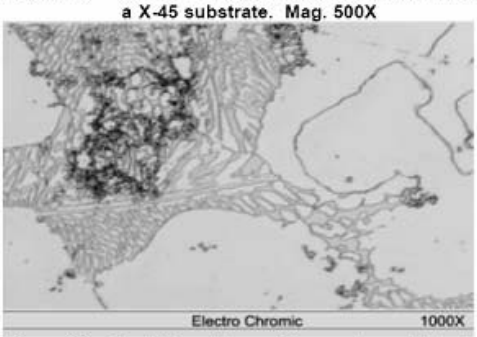

Figure 29 – Traditional type wide gap brazed joint on a X-45 substrate. Mag.1000X

Figure 30 shows an area in the wide gap brazed joint, along the grain boundary, where 3 phases were analysed. The braze area as seen in figure 31, contains Co, Cr, Ni, Ta and W, and the W and Ni percentages are higher than that present in the LPD bonded joints. The 3 phases identified were 2 Ta rich phases as seen in figures 32 and 33 (probably Ta-carbide) and a Cr, W rich phase as seen in figure 34 (probably a Cr, W boride).

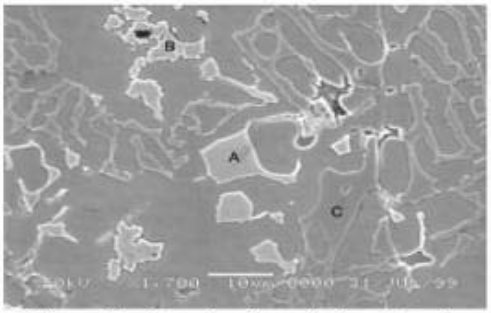

Figure 30 – Area along the grain boundary of a traditional wide gap braze where 3 phases where analysed.

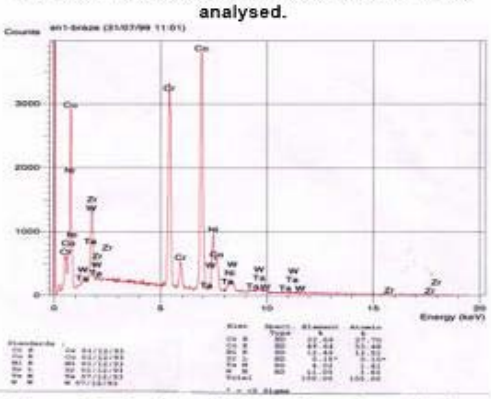

Figure 31 – Semi-qualitative and semi-quantitative analysis of the traditional type wide gap braze.

Figure 32 – Semi-qualitative and semi-quantitative analysis of the phase"A", along the grain boundary of a traditional type wide gap braze.

Figure 33 – Semi-qualitative and semi-quantitative analysis of the phase"B", along the grain boundary of a traditional type wide gap braze.

Figure 34 – Semi-qualitative and semi-quantitative analysis of the phase"C", along the grain boundary of a traditional type wide gap braze.

FIRST ARTICLE REPAIR DEMONSTRATION

An engine run vane with the types of damage shown in fig's 2-6 was obtained. The cracks were ground/routed out and then were repaired using the LPDB process "Sermafill". Figures 35 (a and b), 36 (a and b), 37 (a, and b), 38 (a and b), 39 (a and b), 40 (a and b) and 41 (a, b, c and d) all show the routed cracks and the very same repaired area. The crack in fig 41 is a through wall crack, hence fig's 41(c) and (d) are photographs taken from the opposite side of the through wall crack.

Figure 35(a) – Routed crack

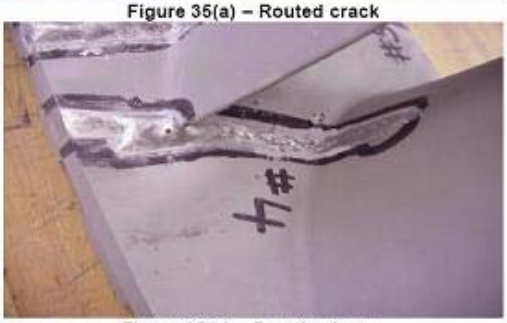

Figure 35(b) – Repaired area

Figure 36(a) – Routed crack

Figure 36(b) – Repaired area

Figure 37(a) – Routed crack

Figure 37(b) – repaired area

Figure 38(a) – Routed crack

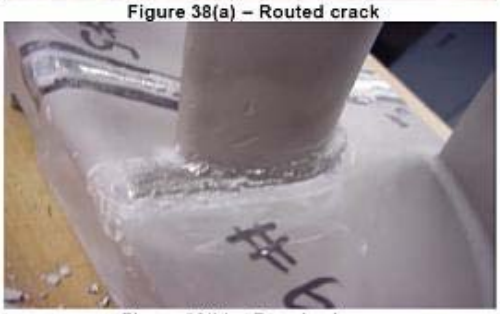

Figure 38(b) – Repaired area

Figure 39(a) – Routed crack

Figure 39(b) – Repaired area

Figure 40(a) – Routed crack

Figure 40(b) – Repaired area

Figure 41(a) – Routed crack

Figure 41(b) – Repaired area

Figure 41 (c) – Repaired area

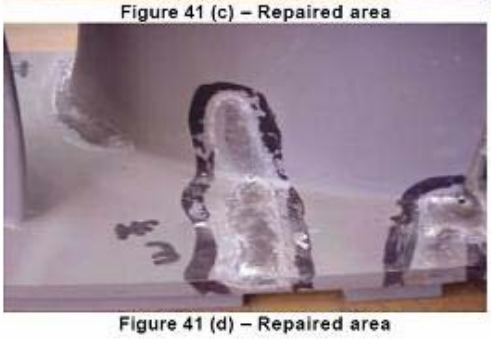

Figure 41 (d) – Repaired area

Figures 42(a) and (b) show the build up of the hook fit areas, which was required because of downstream deflection of the inner buttress/seal areas, as a result of axial creep.

Figure 42(a) – Hook fit restoration, using paste.

Figure 42(b) – Hook fit restoration, using pre-sintered plate.

METALLURGICAL EVALUATION OF FIRST ARTICLE REPAIR DEMONSTRATION

The cracks repaired (in fig's 35 – 41) using the LPDB process, were sectioned and a conventional metallurgical analysis was conducted. Figure 43 shows a macrograph taken through the crack. The paste has filled the complete cavity of the crack and there is good bonding to the sidewalls of the routed out crack. A semi-quantitative and qualitative analyses on the base metal and joint can be seen in fig's 44 and 45. Essentially the elements of Co, Cr, Ni and W were found in the X-45 base metal as seen in figure 44. The LPD bonded repaired joint not only had the same elements as the base metal, (except for Ta, which is present in the chemistry of the "Sermafill" paste) but the elements only differed by 1% when comparing the chemistry of the 2 regions.

Figure 43 – Macrograph taken through a crack repaired with the "Sermafill" process

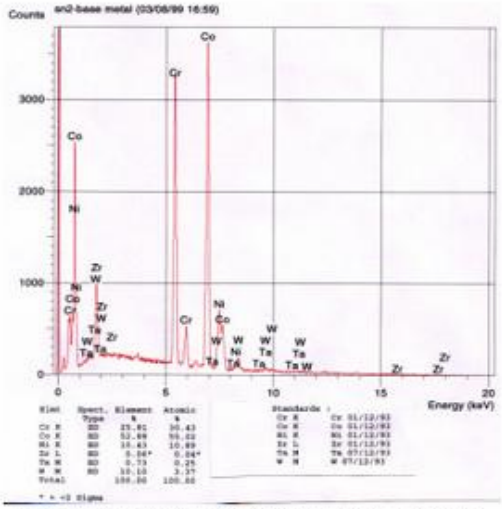

Figure 44 – Semi-qualitative and semi-quantitative analysis of the X-45 base metal.

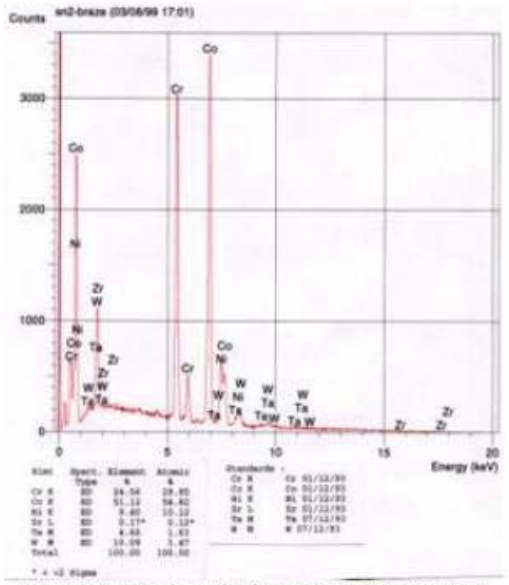

Figure 45 – Semi-qualitative and semi-quantitative analysis of the crack repaired region i.e. the "Sermafill'ed" joint.

Figures 46, 47 and 48 show at different magnifications, the microstructure of the repaired crack region using the "Sermafill" process. The microstructure is similar to that present in figures 11, 12 and 13 or figures 18, 19 and 20.

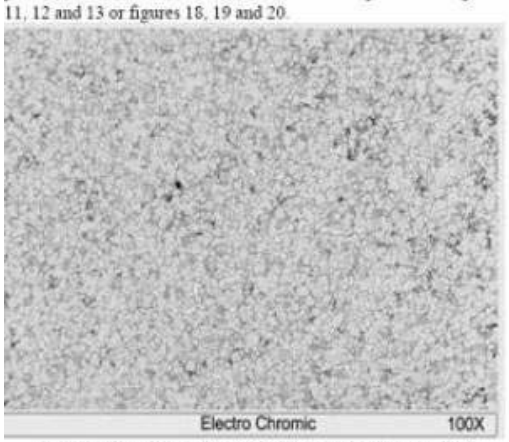

Figure 46 – Microstructure of the crack repaired region using the LPDB/"Sermafill" process. Mag. 100X

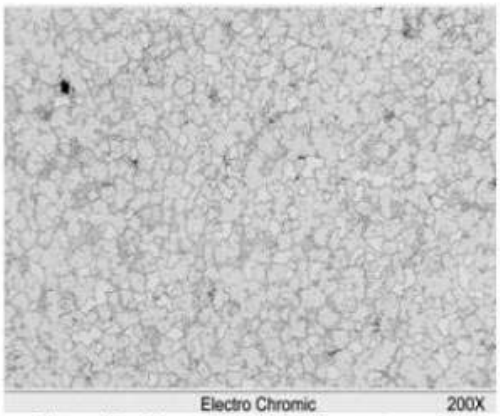

Figure 47 – Microstructure of the crack repaired region using the LPDB/ "Sermafill" process. Mag. 200X

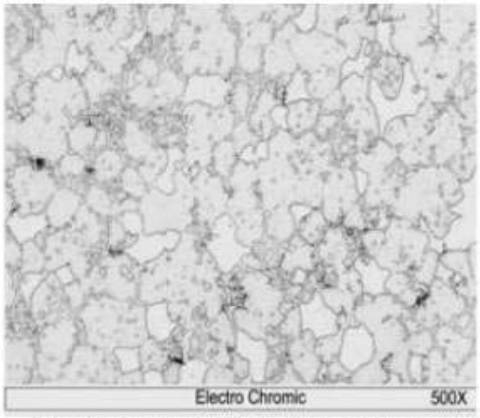

Figure 48 – Microstructure of the crack repaired region using the LPDB/ "Sermafill" process. Mag 500X

The phases seen on the grain boundaries in fig 49, are either W-borides or carbides, and Cr-borides or carbides respectively, as represented in the semi-qualitative and quantitative analyses seen in fig's 50 and 51. As the EDAX system on the SEM could not detect either B or C it was difficult to precisely state the phases that formed in the joint. From the phase morphology it is probably a Cr-carbide phase and W-boride phase that is present in the repaired area.

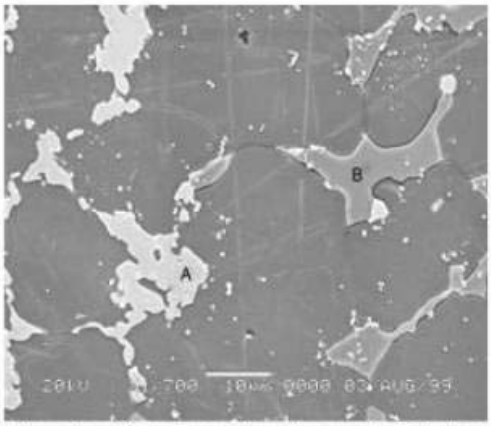

Figure 49 – Phases present on the grain boundaries of a crack repaired area

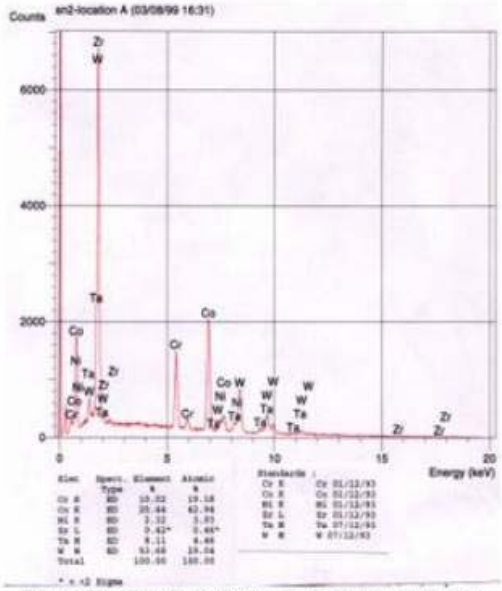

Figure 50 – Semi-qualitative and semi-quantitative analysis of the phase "A", along the grain boundary of a repaired crack using the LPDB/ "Sermafill" process.

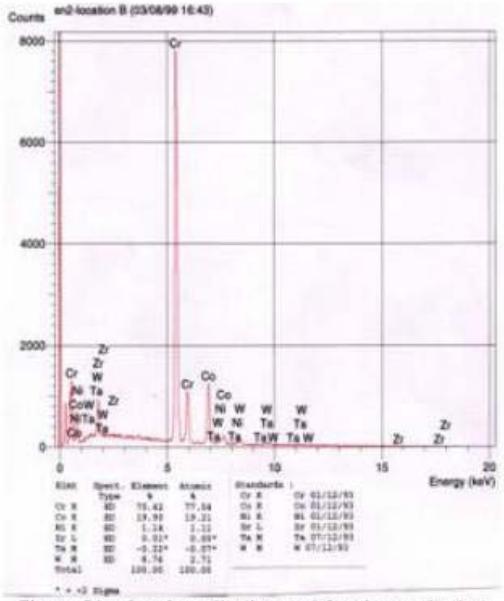

Figure 51 – Semi-qualitative and Semi-quantitative analysis of the phase "B", along the grain boundary of a repaired crack using the LPDB/ "Sermafill" process.

POSSIBLE WORKSCOPE FOR REPAIR OF W501F, ROW 3 VANES

- Incoming inspection for damage
- Inspect cooling holes for damage
- Airflow a percentage of the vanes
- Disassemble the vanes
- Vibropeen appropriate parts
- Rout out cracks and appropriate indications
- Grit blast
- Acetone clean
- Repair all areas including the hook fit region, using the "Sermafill" process. Note this process incorporates a heat treatment at 1150°C (2100°F) for 4 hours
- Blend repaired area to proper contour
- EDM cooling holes
- Inspection
- Heat treat at 982°C (1800°F) for 4 hours
- Blast clean
- Machine vane segments
- Record final dimensions
- Assemble the vanes
- Airflow the vanes
- Final inspection

SUMMARY AND CONCLUSIONS

- The use of the LPDB ("Sermafill") process, results in a repaired joint, which has mechanical properties (tensile and stress rupture) equivalent to that of the base metal.
- The microstructure of the joint shows no signs of large networks of brittle boride phases, known to significantly reduce mechanical properties and ductility. Only isolated boride phases were seen in the repaired area.
- The LPDB process yields superior mechanical properties when comparing with the traditional wide gap brazing process.
- Based on the metallurgical and mechanical results obtained in this in-house research project, the use of the LPDB ("Sermafill") process is a suitable alternative to the traditional Gas Tungsten Arc weld approved repair process specified by the OEM.
- At the time of drafting this document, approval has been granted by the OEM for the LPDB repair of only the hook fit areas of this vane segment. Therefore at this stage the crack repair has nearly completed its developmental stage and is therefore not in production.
- The LPBD ("Sermafill") process is ideally suited for crack repair, wall thickness repair of the convex and concave surfaces and dimensional restoration of the hook fit and race track areas of all Co-based vanes.
- This process also works well on Ni-base superalloy components and this will form the basis of a paper in the near future.

ACKNOWLEDGMENTS

The authors acknowledge the help of Jan Williams and Kevin Pelletier of Dirats Laboratory for the mechanical testing and metallographic work.

REFERENCES

Demo, W.A and Ferrigno, S.J, 1992, "Brazing method helps repair aircraft gas –turbine nozzles", Advanced Materials and Processes, Vol 141, No.3, pp43-45

Wustman, R.D and Smith, J.S, 1996, "High strength diffusion braze repairs for gas turbine components", ASME paper 96-GT-427

Bell, S, 1985, "Repair and Rejuvenation procedures for aero gas-turbine hot section components", Material Science and Technology, Aug, Vol 1, pp629

Ellison, K.A, Lowden, P and Liburdi, J, 1992, "Powder metallurgy Repair of Turbine Components", ASME paper 92-GT-312

AWS Welding Handbook, Vol2, 8th edition, pp380

Metals Handbook, Vol3, 9th edition

APPENDIX B

MIGLIETTI, W.M., KEARNEY, J., AND PABON, L. "LIQUID PHASE DIFFUSION BOND REPAIR OF SIEMENS V84.2, ROW 2 VANES AND ALSTOM TORNADO 2ND STAGE STATOR SEGMENTS". PROCEEDINGS OF THE *ASME TURBO EXPO CONFERENCE 2001*. 2001. NEW ORLEANS, USA.

LIQUID PHASE DIFFUSION BOND REPAIR OF SIEMENS V84.2, ROW 2 VANES AND ALSTOM TORNADO, 2ND STAGE STATOR SEGMENTS

Warren M Miglietti , John Kearney and Luis Pabon
Sermatech International, Inc., Manchester, CT, 06040

ABSTRACT

During the industrial turbine engine operation of the Siemens V84.2, Row 2 vanes, and the Alstom Tornado, 2nd stage stator segments, "craze-cracking" and isolated thermal fatigue cracks develop during engine operation. Other damages found include pitting and dents resulting from corrosion/erosion and FOD (foreign object damage), respectively. Erosion and oxidation damage is also commonly found on the airfoils. This paper describes the vacuum LPDB (liquid phase diffusion bond) repair process used to repair all of the above-mentioned damage.

As a means of qualifying the high temperature diffusion bond process, both metallurgical and mechanical property evaluations were carried out. The metallurgical evaluation consisted of optical and scanning electron microscopy. The wide gap diffusion bonded area consisted of a fine-grained structure with intermetallic phases dispersed both intergranularly and intragranularly. An Energy Dispersive X-ray analysis was also conducted and the results are reported.

The chemistry of the repaired area is similar to the base metal which may explain why mechanical tests revealed properties equivalent to that of the base metal. The mechanical evaluations undertaken were tensile tests at room temperature and elevated temperature, as well as stress rupture tests. These results were equivalent to mechanical properties of the IN738 and IN939 Ni-based superalloys, which is the base metal that the above mentioned vanes and stator segments are manufactured from.

INTRODUCTION

Brazing has been utilised for decades, to repair aircraft engine vane and nozzle segments. It has only been the last five years that a variant of brazing has been utilised for Industrial Gas Turbine (IGT) vane and nozzle repairs. The traditional wide gap brazing process was made popular by GE's and Pratt and Whitney's ADH (activated diffusion healing) (Demo and Ferrigno, 1992) and Turbofix processes respectively. Many repair vendors have their own proprietary wide gap braze process such as SNECMA's RBD (rechargement per brasage diffusion), Howmet's ESR (effective structural repair) (Wustman and Smith, 1996), and Chromalloy's SRB (surface reaction braze) (Bell, 1985). Other wide gap joining processes available are LPDS (liquid phase diffusion sintering), Liburdi's LPM (Liburdi powder metallurgy) (Ellison, Lowden and Liburdi, 1992) and Sermatech's "SermaFill" process. The latter three processes do not comply exactly with the definition of brazing as defined by the American Welding Society (AWS Welding Handbook, Vol. 2). Hence liquid phase diffusion sintering as referred to by Siemens/Westinghouse, powder metallurgy as referred to by Liburdi Engineering and liquid phase diffusion bonding (LPDB) as referred to by Sermatech are relatively new names appearing on the technological list of techniques to repair vanes and nozzles.

The object of this paper is to describe the use of the liquid phase diffusion bonding process, (which Sermatech have as their trademark the SermaFill process) for Siemens V84.2, Row 2 vane and Alstom Tornado 2nd stage stator segment repairs. This SermaFill process was also compared with the traditional wide gap braze process. The former process is proprietary and in the process of being patented, hence exact precise temperatures and times, chemical compositions etc. cannot be revealed in this paper; nevertheless, ranges of temperature and times are reported here.

The LPDB process was qualified by undertaking a metallurgical evaluation and a mechanical property evaluation to show that metallurgically sound and high strength joints resulted. This LPDB process was used to restore wall thickness on the concave and convex surfaces of the airfoil on the 2nd

stage stator segments as well as to repair cracks and pits/dents. The process was also used to repair craze cracking on the Row 2 vanes. Figures 1-4 show typical examples of the cracking on both components. The Row 2 vanes and 2nd stage stator segments are cast from IN738 and IN939, respectively. The nominal composition of IN738 and IN939 is Ni-16Cr-8.5Co-1.75Mo-2.6W-1.75Ta-0.9Nb-3.4Al-3.4Ti-0.1Zr-0.17C and Ni-22.4Cr-19Co-2W-1.4Ta-1Nb-1.9Al-3.7Ti-0.1Zr-0.15C, respectively. These cracks are wide; therefore conventional narrow gap brazing cannot be utilised as a repair technique.

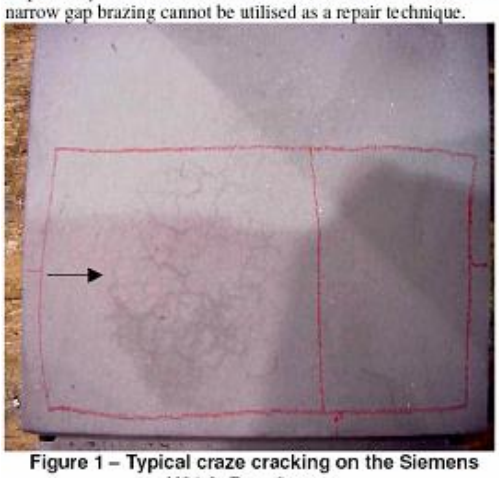

Figure 1 – Typical craze cracking on the Siemens V84.2, Row 2 vane.

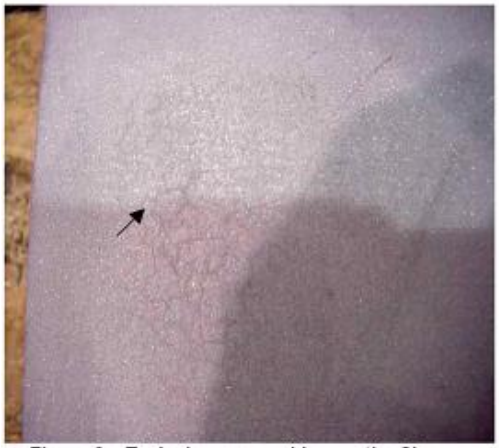

Figure 2 – Typical craze cracking on the Siemens V84.2, Row 2 vane.

The largest width of cracks found on these engine sets was 1.5mm (0.059''). Therefore for the process qualification the mechanical property tests (namely tensile and stress rupture) were undertaken on samples where the joint gap was 1.5mm (0.059''). The process is not limited to this gap and the largest gap repaired to date has been 10mm.

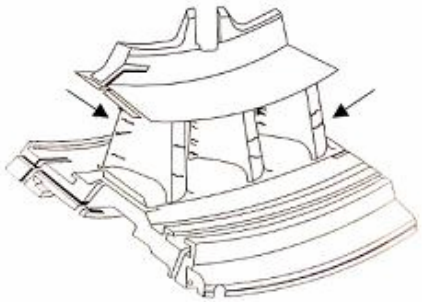

Figure 3 – Typical view from the concave side, showing leading, trailing and shroud/buttress cracking on the Alstom Tornado 2nd stage stator segment.

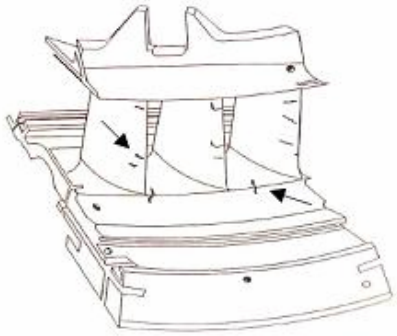

Figure 4 – Typical view from the convex side, showing leading, trailing and shroud/buttress cracking on the Alstom Tornado 2nd stage stator segment.

PROCESS EXPERIMENTAL PROCEDURE

Tensile tests at room temperature (21°C) and elevated temperatures, as well as stress rupture tests were undertaken. The test specimens were prepared in a butt joint configuration as seen in Fig. 5. The joint is in the centre of the gauge length and was 1.5mm wide.

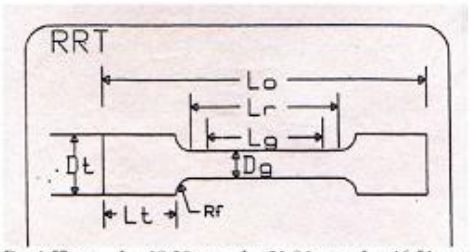

D_g=4.57mm, L_g=18.29mm, L_t=21.84mm, L_o=46.51mm, R_f =3.18mm, D_t=(5/16-24NF-2A inches) and L_t=9.53mm

Figure 5 – Configuration of tensile and stress rupture test specimens

Figure 6 shows the set up for the samples utilised for the metallographic evaluation. Molybdenum sheet stock was utilised to keep the joint gap uniform at 1.5mm in width. Conventional metallographic techniques were used for the metallurgical investigation.

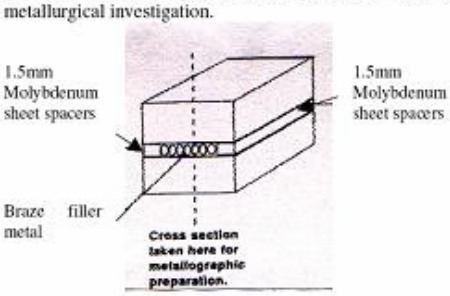

Figure 6 – Schematic representation of sample set for metallurgical evaluation

TENSILE AND STRESS RUPTURE TEST SPECIMEN PREPARATION

Mechanical test specimens according to the configuration shown in Fig. 5 were prepared as follows:

a) Obtain investment cast IN738 and IN939 material.
b) Machine rectangular sections of 12.5mm (0.5'') X 12.5mm (0.5'') X 55.9mm (2.2'')
c) Cut sample in half.
d) Grind the mating surfaces flat.
e) Grit blast surfaces with silicon carbide.
f) Shim gap at 1.5mm (0.059'').
g) Apply paste to the joint gap.
h) Place samples in fixture to maintain alignment.
i) Set in vacuum furnace.
j) Process between 1120°C (2048°F) and 1200°C (2192°F).
k) Isothermally process at the above-mentioned range for 4-20 hours.
l) Age at 843°C (1550°F) for 24hours for IN738 or age at 900°C (1650°F) for 24hours + 700°C (1300°F) for 16 hours for IN939.
m) Machine samples to the configuration shown in Fig. 5.
n) Send the machined specimens for X-ray analysis to determine if porosity greater than 0.4mm (0.016'') exists and for lack of bonding to the mating surfaces.

RESULTS AND DISCUSSION OF MECHANICAL PROPERTY TESTING

Table 1 below shows the results of the tensile tests undertaken at room temperature, and elevated temperatures of 650°C, 760°C and 982°C on the LPDB joints for IN738. As can be seen the tensile and yield strengths are extremely close to the values quoted in the Metals Handbook. The elongation of the LPDB joints appears low, when compared to the values quoted in the Metals Handbook. There is a good explanation for this, which will be discussed later. Nevertheless the RA values are equivalent to the base metals values and hence the joints possess reasonable ductility.

Table 1: Tensile Strength of IN738 processed with "SermaFill"5 Filler Metal

TEMPERATURE		TENSILE STRENGTH		YIELD STRENGTH		ELONGATION	RA
°C	°F	MPa	ksi	MPa	ksi	%	%
21	70	1011	146.5	882	127.8	3.1	4.7
21	70	886	128.4	866	125.5	1.4	3.6
21	**70**	**1050**	**152**	**865**	**125.4**	**5**	**5**
650	1200	827	120	671	97.3	6.0	5.6
650	1200	765	111	661	95.8	3.3	4.0
650	1200	753	109	682	98.9	4.1	3.7
650	**1200**	**850**	**123**	**655**	**95**	**5**	**5**
760	1400	908	131.6	747	108.3	3.9	5.9
760	1400	944	136.8	768	111.3	3.8	5.6
760	**1400**	**965**	**140**	**795**	**115**	**6**	**NR**
982	1800	412	59.7	319	46.2	2.0	8.2
982	1800	372	53.9	317	45.9	1.6	6.1
982	**1800**	**435**	**63**	**325**	**47.1**	**6.5**	**NR**

NOTE: **Values in Bold are for IN738 parent alloy (Metals Handbook Vol.3, ninth edition) NR = Not Reported**

To verify if the elongation is as low as the data indicates, some IN738 material was taken from the root area of a W501F, 1st stage blade. This material was machined to the configuration shown in Fig. 5. Table 2 shows the results of the IN738 specimens removed from the blade root.

As seen in Table 2 the mechanical properties of the IN738 taken from the actual blade casting is lower than that quoted in the Metals Handbook, including the ductility. Therefore the LPDB joints have ductility in the order of 80% of the IN738 casting material. This is acceptable and the 20% loss in ductility is attributed to the few brittle intermetallic phases present in the 1.5mm (0.059'') wide gap joint.

Table 2: Tensile strength of IN738 material taken from the root of a blade

TEMPERATURE		TENSILE STRENGTH		YIELD STRENGTH		ELONGATION	RA
°C	°F	MPa	ksi	MPa	ksi	%	%
21	70	828	120	759	110	3	3
21	**70**	**1050**	**152**	**865**	**125.4**	**5**	**5**

NOTE: Values in Bold are for IN738 parent alloy (Metals Handbook Vol.3, ninth edition)

Table 3 shows the stress rupture properties of the LPDB joints

Table 3: Stress rupture properties of IN738 processed with " SermaFill" 5 Filler Metal

TEMPERATURE		STRESS LEVEL		HOURS TO FAILURE	ELONGATION	RA
°C	°F	MPa	ksi	hrs	%	%
843	1550	345	50	190.3	1.7	NR
843	1550	345	50	93.7	1.9	NR
843	1550	345	50	89	2.3	NR
843	1550	345	50	97.3	1.8	NR
843	**1550**	**345**	**50**	**100**	**5**	**5**
829	1525	345	50	203.37	4.4	NR
829	**1525**	**345**	**50**	**223.02**	**6.7**	**NR**
982	1800	124.2	18	453.2*	5.5	NR
982	**1800**	**124.2**	**18**	**807.2**	**5.2**	**NR**

NOTE: Values in bold are for IN738 material, taken from the root of a blade. NR = Not Reported
* means that failure occurred in the base metal

As seen in Table 3, the stress rupture properties of the joints are a minimum of 89% of the base metals stress rupture properties.

For those readers who prefer the results shown in graphical form, Figs. 7 and 8 show the tensile and Larson Miller stress rupture data of the LPDB joints.

To compare the results of the LPDB wide gap joints with a more traditional wide gap braze process, a 50%IN738 and 50% BRB braze mixture was developed. Some samples were brazed with the same joint gap and at the same process parameters as those of the LPDB joints. The 50% braze used in the mixture had a composition Ni-13.5Cr-7.5Co-4Al-2.5B.

Tables 4 and 5 show the tensile test results and stress rupture results respectively, of the joints brazed with the 50/50 mixture. As seen in these tables the strength of the brazed joint is 40%-53% of the base metal's strength, the elongation is 33-50% of the cast IN738 blade material and the stress rupture life varies from 7.4-11.9% of the parent metals life. This is undesirable if the objective is to have a structural repair, where the properties of the repaired areas are equivalent to the base metal. Clearly the LPDB type joints have superior mechanical properties when compared to a more traditional wide gap braze joint, and the properties are equivalent to the base metal as seen in Tables 1 and 3.

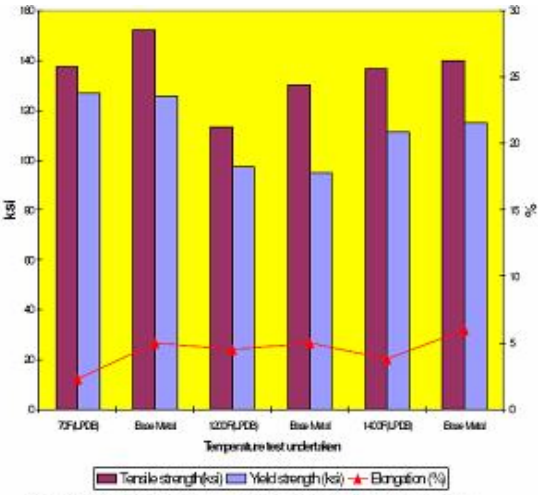

Figure 7 – Tensile properties of the LPDB joints for IN738 Nickel Base superalloy. °C = (°F – 32) / 1.8 MPa = ksi X 6.9

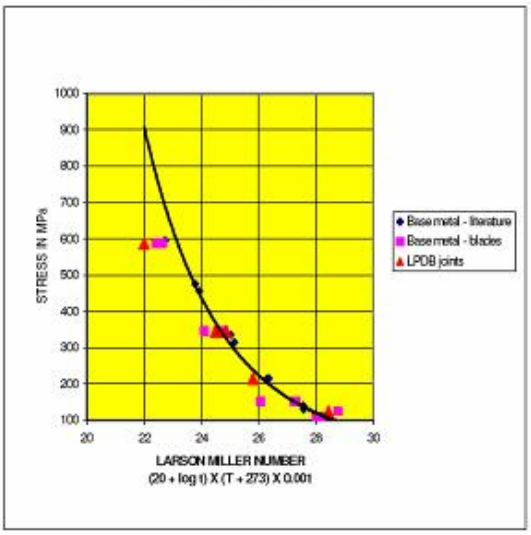

Figure 8 – Larson Miller plot of the stress rupture properties of the LPDB joints for IN738 superalloy.

Table 4: Tensile strength of IN738 brazed with a traditional type filler metal (50%IN738 + 50%BRB)

TEMPERATURE		TENSILE STRENGTH		YIELD STRENGTH		ELONGATION	RA
°C	°F	MPa	ksi	MPa	ksi	%	%
21	70	527	76.4	527	76.4	1.4	2.4
21	70	502	72.8	502	72.8	1.8	2.2
21	70	559	81	559	81	1.0	2.9
21	**70**	**1050**	**152**	**865**	**125.4**	**5**	**5**
650	1200	322	46.7	322	46.7	2.5	1.6
650	1200	441	63.9	441	63.9	1.2	1.9
650	1200	338	49	338	49	1.9	5.2
650	**1200**	**850**	**123**	**655**	**95**	**5**	**5**

NOTE: Values In Bold Are For IN738 Alloy (Metals Handbook Vol.3, ninth edition)

Table 5: Stress Rupture properties of IN738 brazed with a traditional type filler metal (50%IN738 + 50%BRB)

TEMPERATURE		STRESS LEVEL		HOURS TO FAILURE	ELONGATION	RA
°C	°F	MPa	ksi	hrs	%	%
843	1550	345	50	11.9	NR	NR
843	1550	345	50	7.4	NR	NR
843	**1550**	**345**	**50**	**100**	**5**	**5**

NOTE: Values in Bold are for X-45 alloy (Metals Handbook Vol.3, ninth edition) NR = Not Reported

Table 6 and Fig. 9 show the results of the tensile tests undertaken at room temperature and 650°C (1200°F) on the LPDB joints for IN939. As can be seen the tensile and yield strengths are equivalent to the values of the cast material. The elongation of the LPDB joints is 50-73% of the base metals values. This is attributed to the intermetallic phases present in the joint. The RA values are however equivalent to that of the base metal, hence the joints do possess reasonable ductility. As seen in Fig. 10, the stress rupture properties of the joints are a minimum of 90% of the base metal.

Table 6: Tensile Strength of IN939 processed with "SermaFill"3 Filler Metal

TEMPERATURE		TENSILE STRENGTH		YIELD STRENGTH		ELONGATION	RA
°C	°F	MPa	ksi	MPa	ksi	%	%
21	70	920	133.3	670	97.1	2.2	3.6
21	70	859	124.5	696	100.9	1.8	4.3
21	70	817	118.4	750	108.7	1.7	7.7
21	70	999	144.8	651	94.3	1.5	3.0
21	**70**	**897**	**130**	**690**	**100**	**3**	**5.0**
650	1200	768	111.3	625	90.6	1.5	4.0
650	1200	860	124.7	654	94.8	2.1	5.1
650	**1200**	**863**	**125.1**	**621**	**90**	**3**	**5.0**

NOTE: Values in bold are for cast IN939 material taken from a shroud buttress section.

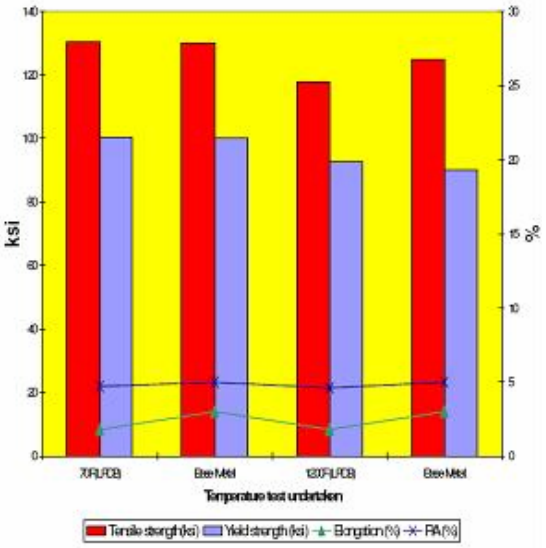

Figure 9 – Tensile properties of the LPDB joints for IN939 Nickel Base superalloy. °C = (°F – 32) / 1.8 MPa = ksi X 6.9

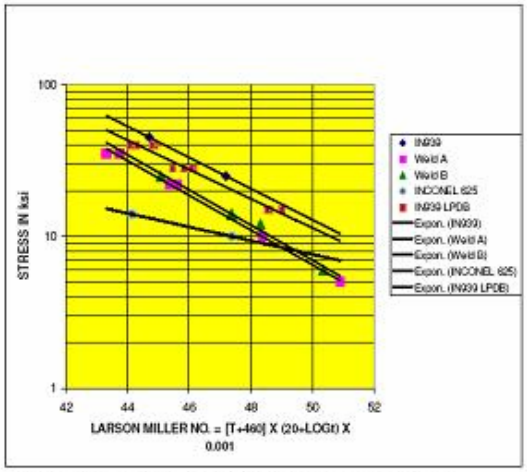

Figure 10 – Larson Miller plot of the stress rupture properties of the LPDB joints for IN939 superalloy. °C = (°F – 32) / 1.8 and MPa = ksi X 6.9

In fact Fig. 10 also shows that the LPDB joints have superior stress rupture lives when compared to three different weld filler metals viz. IN625, Weld A and Weld B. IN625 is well utilised as a filler metal for non-structural repair applications, because of its good ductility and ease of welding. However as can be seen, this filler metal has poor stress rupture life when compared to IN939. Two proprietary higher strength weld filler metals based on the elements Ni-Cr-Co-Mo-W-Ti-Al-C were developed as substitutes for IN625, and even these filler metals, did not even have the stress rupture properties equivalent to those of the LPDB joints.

IN939 as a result of its high Al + Ti content is not readily weldable and suffers from strain age cracking, as seen in Figs. 11 and 12.

Figure 11 – Strain age cracking, on the airfoil, after initial attempts at a weld repair.

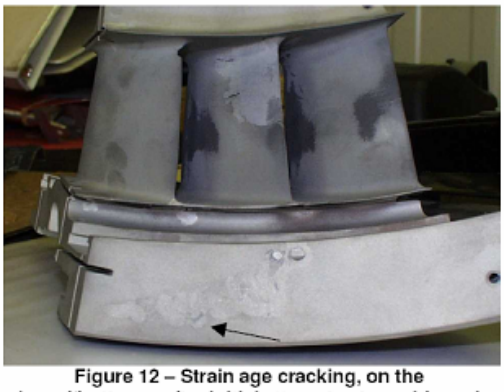

Figure 12 – Strain age cracking, on the shroud/buttress, after initial attempts at a weld repair.

RESULTS AND DISCUSSION OF THE METALLURGICAL EVALUATION

Figure 13 shows the macrograph of a cross section taken through the LPDB repair of the V84.2, row 2 vane. As can be seen the "craze-cracked" area was machined away and this area was filled with the LPDB filler metal.

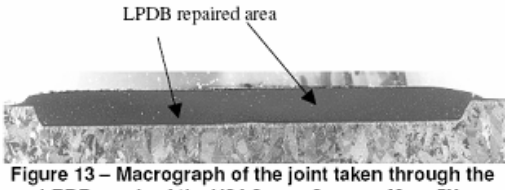

Figure 13 – Macrograph of the joint taken through the LPDB repair of the V84.2, row 2 vane. Mag. 5X

Figures 14 and 15 show the excellent bonding/ adhesion to the vane material. A fine-grained microstructure is evident. Some minor microporosity can be seen in the micrograph, but this microporosity level is considered to be acceptable.

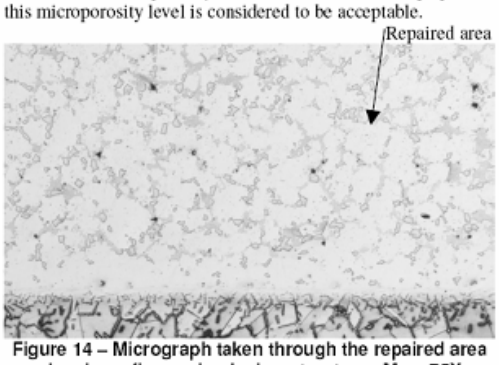

Figure 14 – Micrograph taken through the repaired area showing a fine-grained microstructure. Mag. 75X

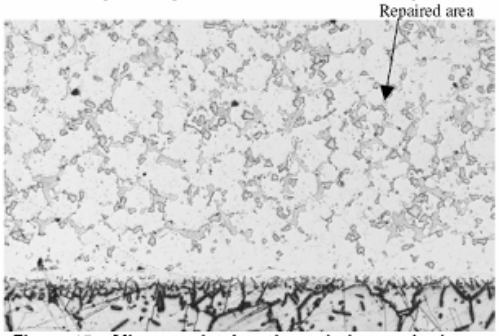

Figure 15 – Micrograph taken through the repaired area showing excellent bonding to the vane material. Mag. 75X

Figures 16 and 17 show the fine-grained structure of the LPDB joint, with intermetallic phases dispersed intergranularly.

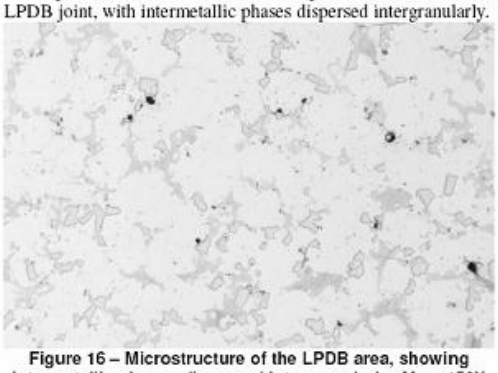

Figure 16 – Microstructure of the LPDB area, showing intermetallic phases dispersed intergranularly. Mag. 150X

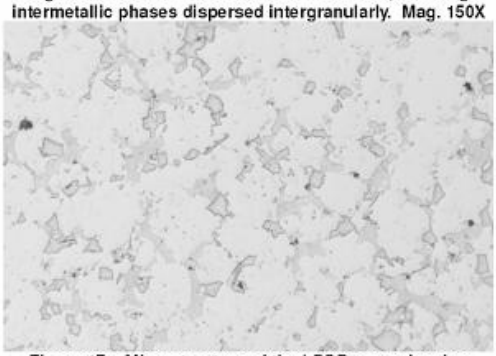

Figure 17 – Microstructure of the LPDB area, showing intermetallic phases dispersed intergranularly. Mag. 150X

Figures 18 and 19 show the intermetallic phases that are present in more detail.

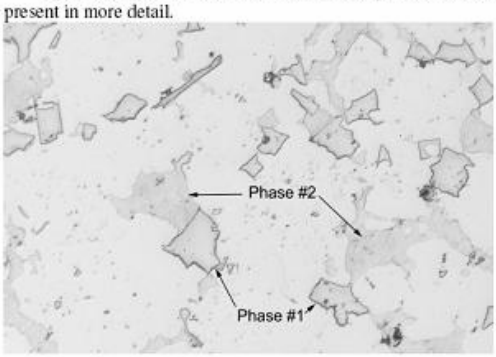

Figure 18 – Intermetallic phases present in the joint. Mag.400X

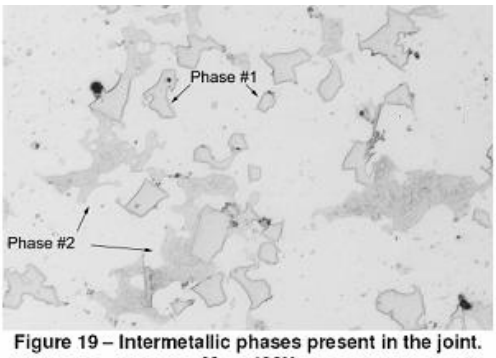

Figure 19 – Intermetallic phases present in the joint. Mag. 400X

Figures 20 and 21 show semi-qualitative analyses of the phases labeled phase #1 and phase #2 in Figs. 18 and 19. Table 7, shows the semi-quantitative analyses of the phases labeled phase #1 and phase #2 in Figs. 18 and 19. As can be seen in Fig. 20 and Table 7, the "blocky" phases #1 are Cr/W rich phases; whereas, the phases #2 are Ni rich phases as seen in Fig. 21 and Table 7. Energy dispersive spectrometry was utilised for this work, and hence neither Boron nor Carbon could be detected. Therefore it is difficult to precisely state what phase is present in the joint. Nevertheless, it is probably a boride or carbide phase that formed. Unfortunately there was no thin window on the EDAX to detect Carbon or Boron.

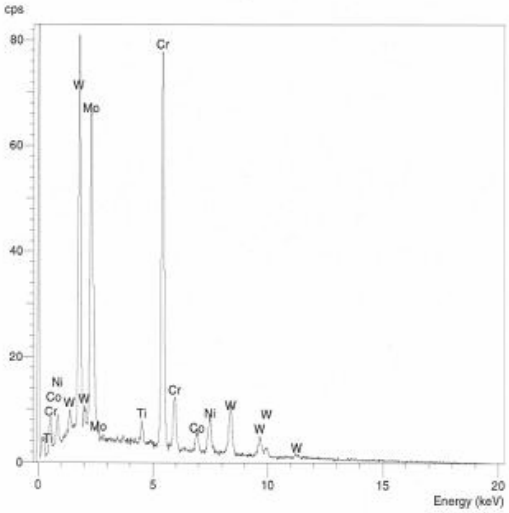

Figure 20 – Semi-qualitative analysis of the phase #1 shown in Figs. 18 and 19.

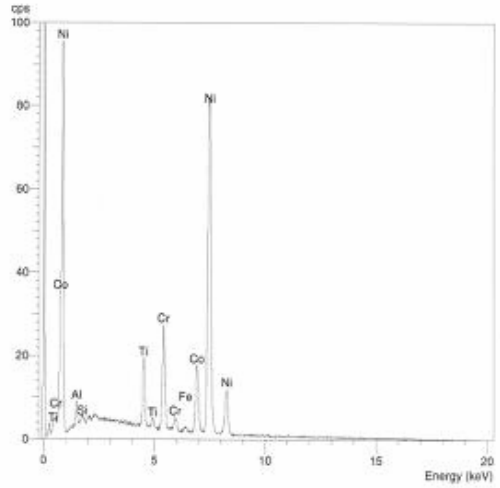

Figure 21 – Semi-qualitative analysis of the phase #2 shown in Figs. 18 and 19

Table 7: Semi-quantitative analysis of the phases present in the joint.

Intermetallic phase	Ni	Cr	W	Mo	Co	Ti	Al
Phase #1	5.4	30.7	30.5	29.0	2.7	1.3	0.5
Phase #2	69.4	10.5	0	0	11.9	5.9	2.1

Figure 22 shows the macrograph of a cross section taken through the LPDB repair of the Tornado 2ad stage stator segment. As can be seen the filler metal has flowed completely down to the bottom of the crack and has bonded excellently to the sidewalls of the routed out crack. Figure 23 shows a cross section taken through a "through" crack at the trailing edge of the airfoil. Once again there is good bonding to the sidewalls of the routed out crack.

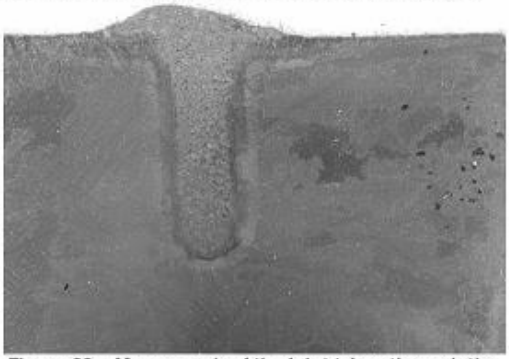

Figure 22 – Macrograph of the joint taken through the LPDB repair of the Tornado, 2nd stage stator segment. Mag. 5X

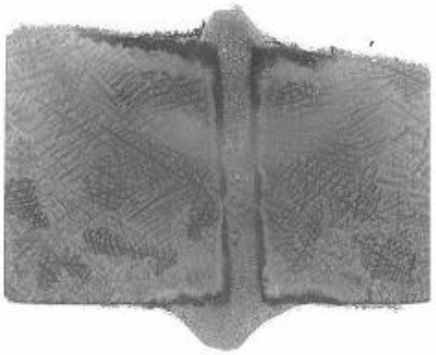

Figure 23 - Macrograph of the joint taken through the LPDB repair of the Tornado, 2nd stage stator segment. Mag. 5X

Figure 24 shows the microstructure of the repaired area. It consists of a fine-grained structure and there is good bonding/adhesion to the sidewalls. The joint interface can be clearly seen in Fig. 25 and there is no lack of sidewall bonding. Figure 26 shows the joint to consist of equiaxed grains with intermetallic phases dispersed intergranularly. These intermetallic phases can be clearly seen in Fig. 27. These "bright blocky" phases were determined to be Cr-rich intermetallic phases as seen in Fig. 28 and Table 8. Energy dispersive spectrometry was utilised for this work, and hence neither Boron nor Carbon could be detected. Therefore it is difficult to precisely state what phase is present in the joint. Nevertheless, it is probably a boride or carbide phase.

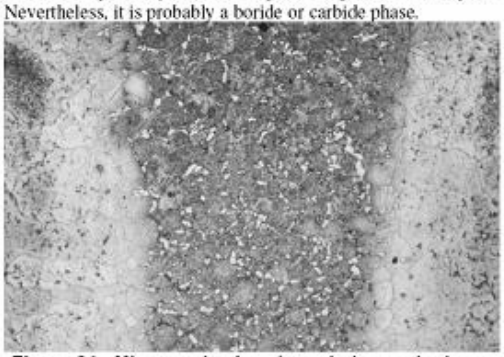

Figure 24 - Micrograph taken through the repaired area showing a fine-grained microstructure. Mag. 45X

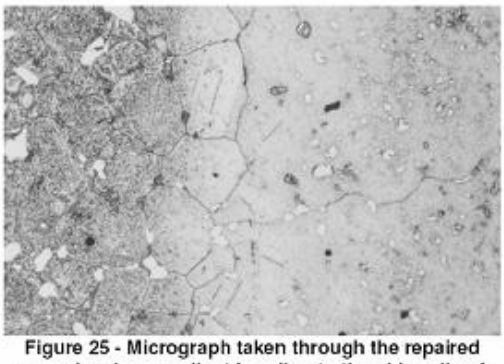

Figure 25 - Micrograph taken through the repaired area showing excellent bonding to the sidewalls of the routed out crack. Mag. 150X

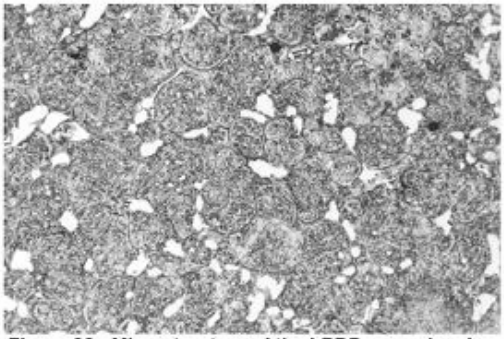

Figure 26 - Microstructure of the LPDB area, showing intergranular intermetallic phases. Mag. 150X

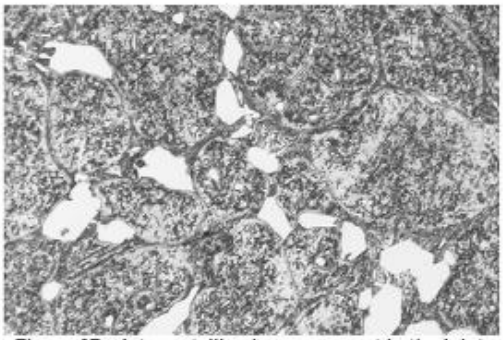

Figure 27 – Intermetallic phases present in the joint. Mag. 400X

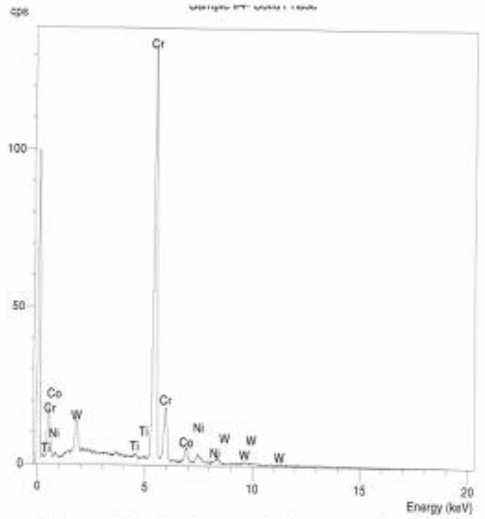

Figure 28 – Semi-quantitative analysis of the intermetallic phases, which are dispersed intergranularly.

Table 8: Semi-quantitative analysis of the phase present in the joint.

Intermetallic phase	Ni	Cr	W	Co	Ti	Al
Intergranular phase	2.7	83.7	8.4	4.7	0.5	0.1

The samples used to produce the mechanical test results shown in Tables 4 and 5, were also analysed. As a reminder a filler metal of 50% IN738 powder and 50%BRB braze was utilised. As seen in Fig. 29 the joint in the stress rupture sample consist of a mixture of fine and coarse grains with a continuous layer of intergranular intermetallic phases. This is in contrast to the discrete isolated and discontinuous intermetallic phases that were present in the joints seen in Figs. 24-27. Figure 30 shows that the traditional type wide gap braze bonded well to the sidewalls of the stress rupture sample and in fact failure did not occur in this region, but through the centre of the joint. Figure 31 shows the continuous intergranular intermetallic phases present in the joint. The bright "blocky and dark grey intermetallic phases can be clearly seen along the grain boundaries. Figure 32 shows these intergranular intermetallic phases more clearly and the phases labeled phase #1 and phase #2 were analysed.

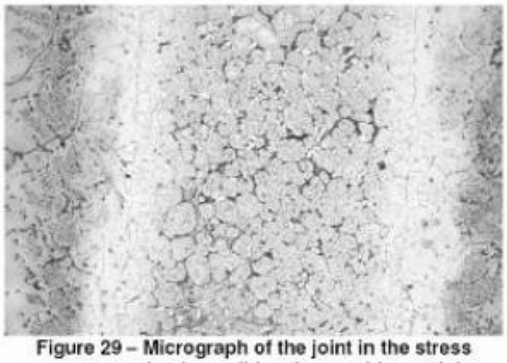

Figure 29 – Micrograph of the joint in the stress rupture sample of a traditional type wide gap joint. Mag. 45X

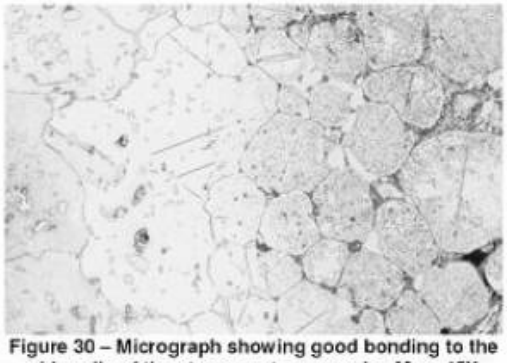

Figure 30 – Micrograph showing good bonding to the sidewalls of the stress rupture sample. Mag. 45X

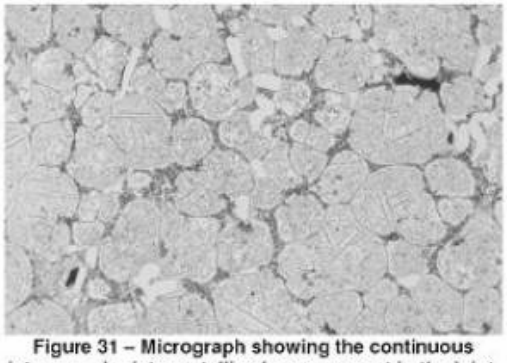

Figure 31 – Micrograph showing the continuous intergranular intermetallic phases present in the joint. Mag. 150X

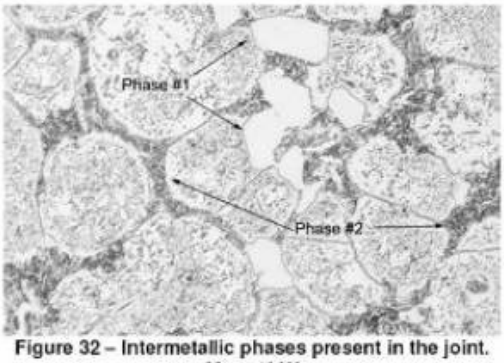

Figure 32 – Intermetallic phases present in the joint. Mag. 400X

Figures 33 and 34 show semi-qualitative analyses of the phases labeled phase #1 and phase #2 in Fig. 32. Table 9, shows the semi-quantitative analyses of the phases labeled phase #1 and phase #2 in Fig. 32. As can be seen in Fig. 33 and Table 9, the "blocky" phases #1 are Cr rich phases; whereas, the phases #2 are Ni rich phases as seen in Fig. 34 and Table 9. Energy dispersive spectrometry was utilised for this work, and hence neither Boron nor Carbon could be detected. Therefore it is difficult to precisely state what phase is present in the joint. Nevertheless, it is probably a boride or carbide phase that formed. Unfortunately there was no thin window on the EDAX to detect Carbon or Boron.

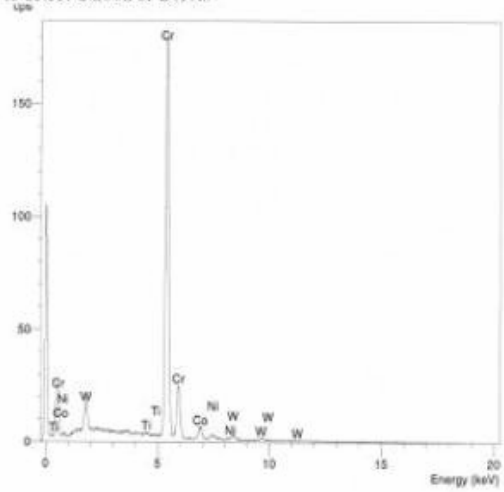

Figure 33 – Semi-qualitative analysis of the phase #1 shown in figure 32.

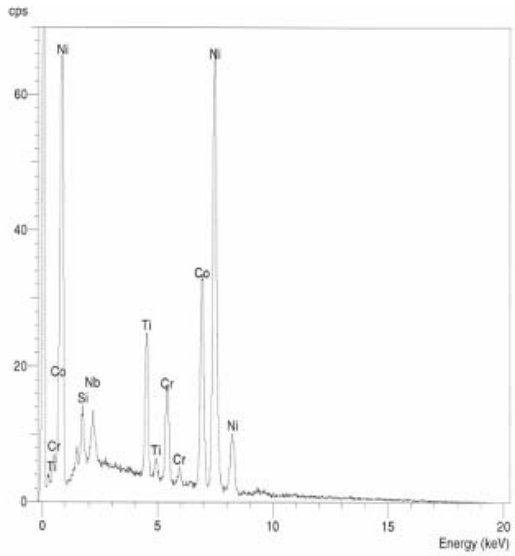

Figure 34 – Semi-qualitative analysis of the phase #2 shown in figure 32.

Table 9: Semi-quantitative analysis of the phases present in the joint.

Intermetallic phase	Ni	Cr	W	Nb	Co	Ti	Al
Phase #1	1.9	85.2	8.3	0	4.3	0.3	0.1
Phase #2	55.5	8.2	0	3.1	25.1	6.3	1.9

FIRST ARTICLE REPAIR DEMONSTRATION

Figures 35 and 36 show areas on the V84.2, row 2 vanes, which were routed out and processed with the LPDB material. Figure 37 shows the V84.2 row 2 vane after complete repair including heat treatment and MCrAlY coating.

Figures 38 and 39 show the Tornado, 2nd stage stator segment after complete repair including heat treatment and Sermaloy J coating. (Sermaloy J is an aluminide coating that is proprietary to Sermatech International, Inc.)

Figure 35 – V84.2, row 2 vanes repaired with the LPDB process.

Figure 36 – V84.2, row 2 vanes repaired with the LPDB process.

Figure 37 - V84.2 row 2 vane after complete repair including heat treatment and MCrAlY coating.

POSSIBLE WORKSCOPE FOR REPAIR OF V84.2 ROW 2 VANES

- Incoming inspection for damage
- Inspect cooling holes for damage
- Airflow a percentage of the vanes
- Disassemble the vanes
- Vibropeen appropriate parts
- Wax mask internal passages and any uncoated external areas
- Strip existing MCrAlY coating
- Grit blast
- Check cooling holes
- Heat tint
- Inspect to ensure that there is no residual coating.
- Measure trailing edge thickness and cooling hole to wall thickness
- FPI
- Rout out indications
- Apply SermaFill 5 filler metal
- Process in vacuum and incorporate the solution heat treat

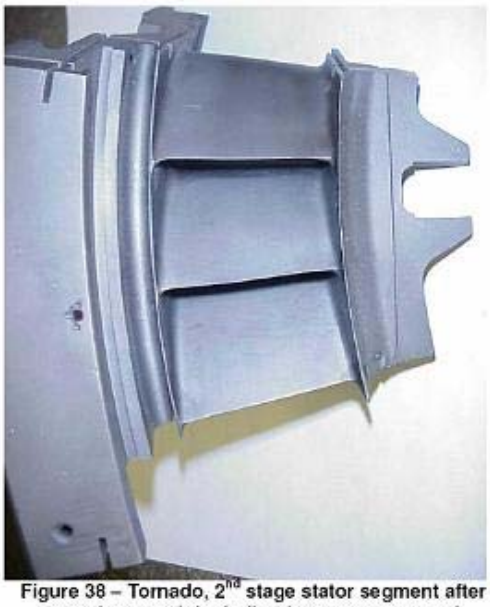

Figure 38 – Tornado, 2nd stage stator segment after complete repair including heat treatment and Sermaloy J coating.

Figure 39 – Tornado, 2nd stage stator segment after complete repair including heat treatment and Sermaloy J coating.

cycle at 2175°F (1191°C) /4hrs
- Blend to proper contour and thickness
- EDM plugged cooling holes
- Apply MCrAlY and TBC coatings
- Diffuse MCrAlY at 2050°F (1121°C) /2hrs
- Age heat treat at 1550°F (843°C) /24hrs
- Install cooling inserts
- Airflow the vanes
- Fixture check
- Final inspection

POSSIBLE WORKSCOPE FOR REPAIR OF TORNADO 2ND STAGE STATOR SEGMENT

- Incoming inspection for damage
- Remove seals and pins
- Grit blast
- Chemically strip
- Heat tint
- Inspect to ensure that there is no residual coating.
- FPI
- Measure trailing edge thickness
- Rout out indications and apply SermaFill 3 filler metal
- Process in vacuum and incorporate the solution heat treat cycle at 2120°F (1160°C) /4hrs
- Blend to proper contour and thickness
- Stabilisation and age at 1830°F (1000°C) /6hrs + 1650°F (900°C) /24hrs
- Apply Sermaloy J coatings
- Diffuse Sermaloy J coating at 1600°F (871°C) /2hrs
- Final age heat treat at 1300°F (704°C) /16hrs
- Install seals and pins if needed
- Airflow the vanes
- Fixture check
- Final inspection

OVERALL DISCUSSION

The results of the mechanical tests showed that the tensile strength values of the LPDB joints on both the IN738 and IN939 base metals, were a minimum of 85% of the base metals tensile strength. The yield strength was equivalent to that of the base metal. The elongation values varied from 30% - 100% of those of the base metal. The RA values varied from 60% - 100% of those of the base metal. The loss in elongation is attributed to the intermetallic phases present in the joint. The stress rupture properties were a minimum of 90% of the base metals properties. Based on the mechanical properties achieved in this study, the use of the LPDB process is considered to be suitable for structural repairs on both the V84.2, row 2 vane and Tornado, 2nd stage stator segment.

The mechanical tests undertaken showed that the traditional type wide gap joints had tensile properties approximately half of the base metals value and stress rupture properties of approximately 10% of the base metals properties. Therefore the use of this type of wide gap filler metal is considered to be unsuitable for 1.5mm wide defects and structural repairs. This type of traditional wide gap braze repair should be confined to non-structural applications.

The LPDB joints consisted of a fine-grained microstructure, with discrete intergranular intermetallic phases. For the IN738 base metal, Cr/W and Ni-rich intermetallic phases existed; whereas, for the IN939 base metal, Cr-rich intermetallic phases existed.

The traditional wide gap braze joints consisted of a mixture of fine and coarse grains. There were continuous intergranular intermetallic phases present, which were Cr and Ni-rich.

First article production repairs showed no coating/bonding interactions.

CONCLUSIONS

- The LPDB ("SermaFill") process, produces a repaired joint having mechanical properties (tensile and stress rupture) equivalent to those of the base metal.
- The microstructure of the joint was found to reveal no signs of large networks of brittle boride phases, known to significantly reduce mechanical properties and ductility. Only isolated and discrete intermetallic phases were seen in the repaired area.
- The LPDB process yields superior mechanical properties when comparing with the traditional type wide gap brazing process.
- Based on the metallurgical and mechanical results obtained in this in-house research project, the use of the LPDB ("SermaFill") process is a suitable alternative to the traditional Gas Tungsten Arc weld approved repair process.
- The LPBD ("SermaFill") process is ideally suited for crack repair, including "craze cracking", wall thickness repair of the convex and concave surfaces and dimensional restoration of the Siemens V84.2, row 2 vane and Alstom Tornado, 2nd stage stator segment.

ACKNOWLEDGMENTS

The authors acknowledge the help of Jan Williams and Kevin Pelletier of Dirats Laboratory for the mechanical testing and metallographic work.

REFERENCES

Demo, W.A and Ferrigno, S.J, 1992, "Brazing method helps repair aircraft gas –turbine nozzles", Advanced Materials and Processes, Vol. 141, No.3, pp43-45

Wustman, R.D and Smith, J.S, 1996, "High strength diffusion braze repairs for gas turbine components", ASME paper 96-GT-427

Bell, S, 1985, "Repair and Rejuvenation procedures for aero gas-turbine hot section components", Material Science and Technology, Aug, Vol. 1, pp629

Ellison, K.A, Lowden, P and Liburdi, J, 1992, "Powder metallurgy Repair of Turbine Components", ASME paper 92-GT-312

AWS Welding Handbook, Vol2, 8th edition, pp380

Metals Handbook, Vol3, 9th edition

APPENDIX C

MIGLIETTI, W.M.A. "WIDE GAP DIFFUSION BRAZE REPAIR OF CO-BASED INDUSTRIAL TURBINE VANES". PROCEEDINGS OF THE *INTERNATIONAL BRAZING & SOLDERING CONFERENCE*. 2-5 APRIL 2000. ALBUQUERQUE, NEW MEXICO, USA. PP. 476-485.

WIDE GAP DIFFUSION BRAZE REPAIR OF Co-BASED INDUSTRIAL TURBINE VANES

W.M.A. Miglietti*

ABSTRACT

During the industrial turbine engine operation, cracks develop on the vanes as a result of thermal fatigue. Other damage found is pitting and dents resulting from corrosion/oxidation and FOD (foreign object damage) respectively. Erosion damage is also commonly found on the airfoils. Finally there is downstream deflection of the inner buttress/seal areas, as a result of axial creep. This paper describes the vacuum wide gap diffusion brazing repair process used to repair all of the above-mentioned damage, including braze build up and machining of the hook fit areas.
As a means of qualifying the high temperature diffusion braze process, both metallurgical and mechanical property evaluations were carried out. The metallurgical evaluation consisted of optical and scanning electron microscopy. The wide gap diffusion brazed area consisted of a fine-grained structure with carbide and boride phases dispersed both intergranularly and intragranularly. An EDAX analysis was also conducted and the results are reported. The microstructure of the repaired area is similar to the base metal which may explain why mechanical tests revealed properties equivalent to that of the base metal. The mechanical evaluations undertaken were tensile tests at room temperature and elevated temperature, as well as stress rupture tests. These results were equivalent to mechanical properties of the X-45, X-40, and FSX-414 Co-based superalloys, which are the base metals that many of the vanes are cast from.

KEYWORDS

Wide Gap Diffusion Brazing, Repair of Industrial Gas Turbine Vanes, Co-based superalloys

INTRODUCTION

Narrow gap brazing has been utilized for decades now to repair aircraft engine vane and nozzle segments. It has only being the last 5 years that wide gap brazing has been utilized for Industrial Gas Turbine (IGT) vane and nozzle repairs. The wide gap brazing process was made popular by GE's and Pratt and Whitney's ADH (activated diffusion healing) by Demo and Ferrigno, 1992 (Ref 1) and Turbofix processes respectively. Many repair vendors have their own proprietary wide gap braze process such as SNECMA's RBD (rechargement per brasage diffusion), Howmet's ESR (effective structural repair) by Wustman and Smith, 1996 (Ref 2) and Chromalloy's SRB (surface reaction braze) by Bell, 1985 (Ref 3). Other wide gap joining processes available are LPDS (liquid phase diffusion sintering), Liburdi's LPM (Liburdi powder metallurgy) by Ellison, Lowden and Liburdi, 1992 (Ref 4) and Sermatech's "Sermafill" process.

*Sermatech International, Inc., 1366 Tolland Turnpike, Manchester, CT, 06040

The objective of this paper is to describe the use of an alternative wide gap braze process for IGT vane repairs, and to compare this process with the traditional wide gap braze process. A traditional wide gap process is referred to as, when a mixture/blend of superalloy powder and braze powder is utilized. The mixtures are usually a 40/60, 50/50 or a 60/40 blend by weight. The alternative wide gap process is proprietary and hence exact precise temperatures and times, chemical compositions etc. cannot be documented; nevertheless, ranges of temperature and times are documented. This process was qualified by undertaking a metallurgical evaluation and a mechanical property evaluation to show that metallurgically sound and high strength joints resulted. This alternative process was used to restore wall thickness on the concave and convex surfaces of the airfoil, repair cracks, pits/dents and build up the hook fit areas, because of downstream deflection of the inner buttress/seal areas, as a result of axial creep.

Many of the IGT vanes are manufactured from Co-based alloys like X-40, X-45 and FSX 414. The chemical composition of the materials is given in Table 1. The high Cr content contributes to corrosion, low temperature oxidation and sulphidation resistance. Figures 1, 2 and 3 show typical examples of ground out cracks on an X-45, W501F, Row 3 vane with 3 airfoils and an FSX-414, GE Frame7EA, Row 1 vane with 2 airfoils. The largest width of crack found on these engine sets was 3.2mm (0.125''), although after grinding through the cracks with grinding discs and burrs, the crack length can vary in width from 6mm-15mm (0.236''--0.600"). As a result of these large gaps, conventional narrow gap brazing cannot be utilised as a repair technique. The hook fit area, which needs to be rebuilt, is shown in Figure 4. For the crack repair, paste is used as the medium for the repair; whereas, with the hook fit repair a tape is utilized.

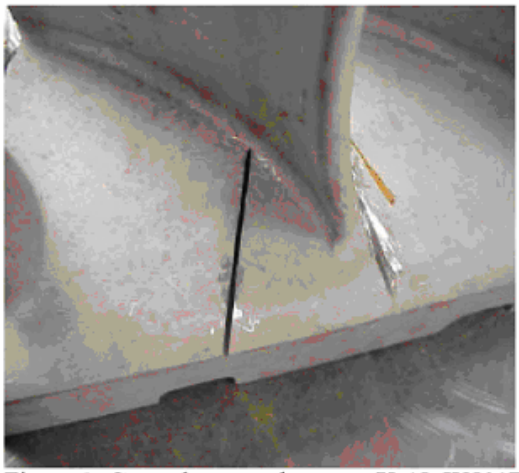

Figure 1: Ground out cracks on an X-45, W501F, Row 3 vane.

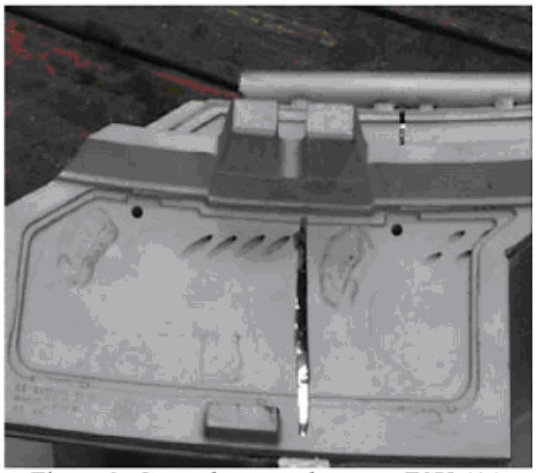

Figure 2: Ground out cracks on an FSX-414, GE Frame 7EA vane.

Element	C	Cr	Ni	W	B	Fe	Si	Zr	Co
X-40	0.5	25	10	7.5	0	1.5	0.4	0.17	Bal
X-45	0.25	25.5	10.5	7	0.012	2 max	0	0	Bal
FSX-414	0.25	29.5	10.5	7	0.012	2 max	0	0	Bal

Table 1: Nominal chemical compositions of some common Co-based superalloys.

Figure 3: Ground out cracks on an X-45, W501F, Row 3 vane.

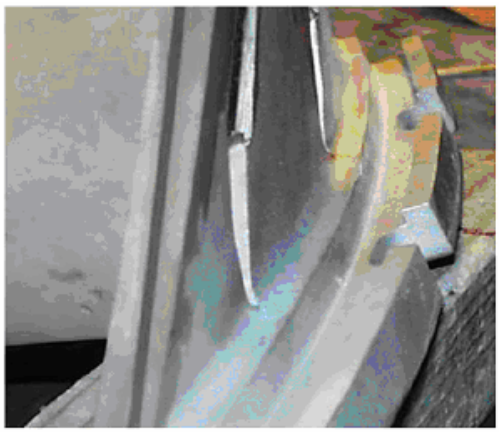

Figure 4: Hook fit area, which need to be built up.

EXPERIMENTAL PROCEDURE

Tensile tests at room temperature and elevated temperature, as well as stress rupture tests were undertaken. The test specimens were prepared in a butt joint configuration as seen in Figure 5. The joint is in the center of the gauge length and is 3.2mm wide. Conventional metallographic techniques were utilised for the metallurgical evaluation. For the traditional type wide gap joints a mixture of 60%Co-based powder (X-40 or X-45) and 40% Co-40Ni-24.5Cr-3B was utilised.

Tensile and Stress Rupture Test Specimen Preparation

Mechanical test specimens according to the configuration shown in Figure 5 were prepared as follows:

a) Obtain scrap vane and cut/grind away sections from the shroud area of the vane.
b) Machine rectangular sections of 12.5mm (0.5'') X 12.5mm (0.5'') X 55.9mm (2.2'')
c) Cut sample in half.
d) Grind the mating surfaces flat.
e) Grit blast surfaces with silicon carbide.
f) Shim gap at 3.2mm (0.125'').
g) Apply paste to the joint gap.
h) Place samples in fixture to maintain alignment.
i) Set in vacuum furnace.
j) Process between 1120°C (2048°F) and 1200°C (2192°F).
k) Isothermally process at the above-mentioned range for 4-20 hours.
l) Age at 982°C (1800°F) for 4hours.
m) Machine samples to the configuration shown in Figure 5.
n) Send machined specimens for X-ray to determine if porosity greater than 1.3mm (0.050'') and for lack of bonding to the mating surfaces exist.

Figure 5: Configuration of Tensile and Stress rupture Test Specimens

RESULTS

Tensile and Stress Rupture Results of the Traditional Type Wide Gap Brazed Joints Base Metal is X-40

Table 2 shows the tensile results of the wide gap joints brazed with 60%X-40/40%braze alloy, where the braze composition was Co-40Ni-24.5Cr-3B.

Temperature		Tensile Strength		Yield Strength		Elongation	RA
°C	°F	MPa	ksi	MPa	ksi	%	%
21	70	555.5	80.5	466.4	67.6	2.6	3.3
21	70	554.1	80.3	437.5	63.4	2.8	2.4
21	70	531.3	77.0	444.7	64.3	3.4	4.8
21	**70**	**745**	**108**	**525**	**76**	**9**	**?**
540	1004	405	58.7	254.6	36.9	3.1	2.6
540	1004	411.9	59.7	253.9	36.8	3.5	2.2
540	1004	380.9	55.2	285	41.3	4.9	1.9
540	1004	391.2	56.7	300.3	43.5	2.1	1.7
540	**1004**	**550**	**79.7**	**275**	**40**	**17**	**?**
650	1200	381.6	55.3	216.7	31.4	6.3	3.1
650	1200	391.2	56.7	216.7	31.4	3.4	1.7
650	1200	400.2	58	228.4	33.1	3.7	2.3
650	1200	393.3	57	227.7	33	3.6	2.2
650	**1200**	**515**	**74.6**	**260**	**38**	**12**	**?**

Table 2. Tensile test results of a wide gap joint brazed with a 60/40 ratio of superalloy powder/braze alloy.
Note: Values in bold are for X-40 base metal taken from the Metals Handbook. (Ref 5)
? means that the RA value was not measured.

As seen in Table 2, the tensile strength of the traditional type wide gap joints is only 70-80% of the base metals strength. Table 3 shows the stress rupture results of the above mentioned joints.

Temperature		Stress Level		Hours to Rupture	Elongation
°C	°F	MPa	ksi	hrs	%
760	1400	260	38	61.4	?
760	1400	260	38	58.2	?
760	**1400**	**260**	**38**	**100**	**?**

Table 3. Stress rupture results of a wide gap joint brazed with a 60/40 ratio of superalloy powder/braze alloy.
Note: Values in bold are for X-40 base metal taken from the Metals Handbook. (Ref 5)
? means that the elongation value was not measured.

As seen in Table 3, the stress rupture strength of the traditional type wide gap joints is typically only 60% of the base metals stress rupture strength. Therefore based on the results in Tables 2 and 3, the traditional type wide gap brazed joints cannot be utilised for high strength repairs, where properties close or equivalent to the base metal is desirable.

Tensile and Stress Rupture Results of the Alternative Type Wide Gap Brazed Joints Base Metal is X-40

Table 4 shows the tensile results of the alternative type, wide gap brazed joints.

Temperature		Tensile Strength		Yield Strength		Elongation	RA
°C	°F	MPa	ksi	MPa	ksi	%	%
21	70	701.4	101.6	508.6	73.7	2.4	3.8
21	70	738.3	107.0	490.7	71.1	2.0	3.4
21	**70**	**745**	**108**	**525**	**76**	**9**	**?**
540	1004	520	75.4	260.3	37,7	2.1	?
540	1004	539.8	78.2	259.9	37.6	2.0	?
540	**1004**	**550**	**79.7**	**275**	**40**	**17**	**?**
650	1200	450	65.2	341	49.4	2.9	3.9
650	1200	509	73.8	311	45.1	6.2	7.8
650	1200	451	65.4	315	45.7	3.6	3.6
650	1200	448	64.9	311	45.1	3.3	3.1
650	**1200**	**515**	**74.6**	**260**	**38**	**12**	**?**

Table 4. Tensile test results of the alternative type wide gap brazed joints.
Note: Values in bold are for X-40 base metal taken from the Metals Handbook. (Ref 5)
? means that the RA value was not measured.

As seen in Table 4, the tensile strength of the alternative type wide gap brazed joints is 87-99% of the base metals strength. Table 5 shows the stress rupture results of the above mentioned joints.

Temperature		Stress Level		Hours to Rupture	Elongation
°C	°F	MPa	ksi	hrs	%
760	1400	260	38	92	?
760	1400	260	38	97.1	?
760	**1400**	**260**	**38**	**100**	**?**

Table 5. Stress Rupture test results of an alternative type wide gap brazed joint.
Note: Values in bold are for X-40 base metal taken from the Metals Handbook. (Ref 5)
? means that the elongation value was not measured.

As seen in Table 5, the stress rupture strength of the alternative type wide gap brazed joints is typically 92-97% of the base metals stress rupture strength. As can be seen comparing the data in Tables 2 and 3, with those of Tables 4 and 5, it can be concluded that the alternative type wide gap brazed joints yield significantly higher tensile and stress rupture strengths, when comparing with the traditional type wide gap brazed joints.

Tensile and Stress Rupture Results of the Alternative Type Wide Gap Brazed Joints Base Metal is FSX-414

Table 6 shows the tensile test results of the alternative type, wide gap brazed joints. The base metal is FSX-414.

Temperature		Tensile Strength		Yield Strength		Elongation	RA
°C	°F	MPa	ksi	MPa	ksi	%	%
21	70	659	95.5	502	72.8	5.5	4.1
21	70	628	91	474	68.7	3.3	16.8
21	70	688	99.7	489	70.9	6.1	13.8
21	**70**	**740**	**107**	**440**	**64**	**11**	**?**
650	1200	503*	72.9	253	36.7	11.4	4.5
650	1200	441*	63.9	274	39.7	8.1	4.8
650	1200	498*	72.2	288	41.7	8.5	7.8
650	**1200**	**485**	**70**	**215**	**31**	**15**	**?**
870	1600	324*	47	311	45.1	25.1	51.9
870	1600	338*	49	233	33.8	31	54
870	1600	330*	47.8	255	37	26.1	49
870	**1600**	**310**	**45**	**165**	**24**	**23**	**?**

Table 6. Tensile test results of the alternative type wide gap brazed joints.
Note: Values in bold are for FSX-414 base metal taken from the Metals Handbook. (Ref 5)
? means that the RA value was not measured. * means failure occurred in the base meta

As seen in Table 6, the tensile strength of the alternative type wide gap brazed joints at roo temperature is 85-93% of the base metals strength. However, at test temperatures above roo temperature failure occurred in the base metal. This implies that the brazed joints at elevat temperature have tensile properties equivalent to the FSX-414 base metal.

Tensile and Stress Rupture Results of the Alternative Type Wide Gap Brazed Joints Base Metal is X-45

Table 7 shows the tensile results of the alternative type, wide gap brazed joints.

Temperature		Tensile Strength		Yield Strength		Elongation	RA
°C	°F	MPa	ksi	MPa	ksi	%	%
21	70	773*	112.0	505	73.2	4.5	1.6
21	70	763*	110.6	531	77	4.4	1.6
21	**70**	**745**	**108**	**525**	**76**	**8**	**?**
650	1200	520*	75.4	304	46.8	6.4	7.1
650	1200	446	64.6	306	44.3	3.1	4.3
650	**1200**	**515**	**74.6**	**260**	**38**	**12**	**?**
760	1400	509*	73.8	311	45.1	2.9	3.9
760	1400	451*	65.4	315	45.7	3.6	3.6
760	1400	450*	65.2	341	49.4	2.9	3.9
760	1400	448*	64.9	311	45.1	3.3	3.1
760	**1400**	**485**	**70**	**?**	**?**	**9**	**?**
980	1800	214*	31	128.4	18.6	4.9	11
980	**1800**	**200**	**29**	**?**	**?**	**16**	**?**

Table 7. Tensile test results of the alternative type wide gap brazed joints.
Note: Values in bold are for X-45 base metal taken from the Metals Handbook. (Ref 5)
? means that the RA value was not measured. *means failure occurred in the base metal.

As seen in Table 7, the tensile strength of the alternative type wide gap brazed joints is superior to that of the base metal, since fracture occurred in the base metal. In many cases the tensile and yield strengths were higher than that quoted in the Metals Handbook and the elongation values were lower than that quoted in the Metals Handbook.

To verify if the elongation is as low as the data indicated, some X-45 material was removed from the shroud area of an actual service exposed W501, Row 3 vane. This material was machined to the configuration shown in Figure 5. The material was then heat treated at 1150°C (2100°F) for 4hours + 982°C (1800°F) for 4hours. Table 8 shows the result of the tensile tests of the X-45 material removed from the vane.

Temperature		Tensile Strength		Yield Strength		Elongation	RA
°C	°F	MPa	ksi	MPa	ksi	%	%
21	70	738	107	514	74.5	5.6	5.6
21	**70**	**745**	**108**	**525**	**76**	**8**	**?**

Table 8. Tensile strength of X-45 material taken from the vane and heat treated.
Note: Values in bold are for X-45 base metal taken from the Metals Handbook. (Ref 5)
? means that the RA value was not measured.

As seen in Table 8, the mechanical properties of X-45, taken from the actual vane casting, is lower than that quoted in the Metals Handbook, especially the ductility. Therefore the alternative type wide gap brazed joints have ductility in the order of 80% of the X-45 casting material. This is acceptable and the 20% loss in ductility is attributed to the few brittle boride phases present in the joint.

Table 9 shows the stress rupture test results for the above alternative type wide gap joints on an X-45 substrate.

Temperature		Stress Level		Hours to Rupture	Elongation	RA
°C	°F	MPa	ksi	hrs	%	%
760	1400	193.2	28	513.9*	31.7	48.3
760	1400	193.2	28	566.5*	29.1	48.1
760	1400	193.2	28	507.1*	35.2	48.5
871	1600	103.5	15	365*	27.7	34.5
871	1600	103.5	15	344.2*	16.4	33.6
871	1600	103.5	15	336.3*	20.7	32

Table 9. Stress Rupture test results of an alternative type wide gap brazed joint.
Note: *means that failure occurred in the base metal.

As seen in Table 9, the stress rupture strength of the alternative type wide gap brazed joints is superior to that of the base metal, since all of the fracture occurred in the base metal.

Figure 6 shows the Larson Miller plot of the alternative type wide gap brazed joints. As can be seen the stress rupture strengths of the joint lie within the scatterband of the base metals rupture strength.

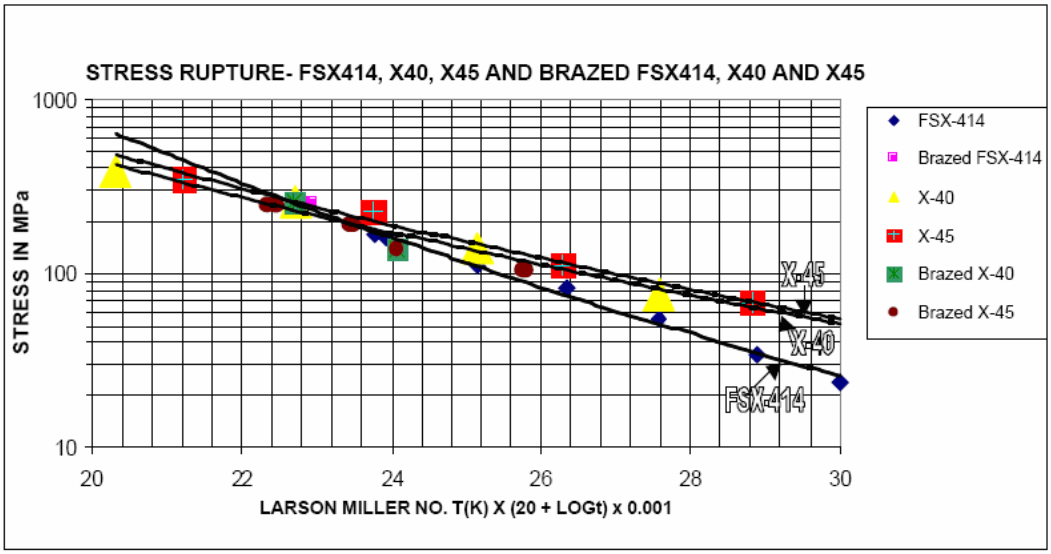

Figure 6: Stress Rupture plot of the brazed joints and base metal for X-45, X-40 and FSX-414.

Metallurgical Results
Traditional Type Wide Gap Brazed Joints

Figures 7 and 8 shows the microstructure of the traditional type wide gap brazed joint on an X-45 base metal. The X-45 powder particles are surrounded with a network of elongated brittle boride phases. This network of brittle boride phases in the wide gap joint, is the predominant reason for the reduction in mechanical properties, including elongation. Figure 9 shows an area in the wide gap brazed joint, along the grain boundary, where 3 phases were analysed. The 3 phases identified were 2, Ta-rich phases (probably Ta-carbide) and a Cr-W rich boride phase as seen in Table10. (The EDAX system on the SEM could not detect the elements C and B).

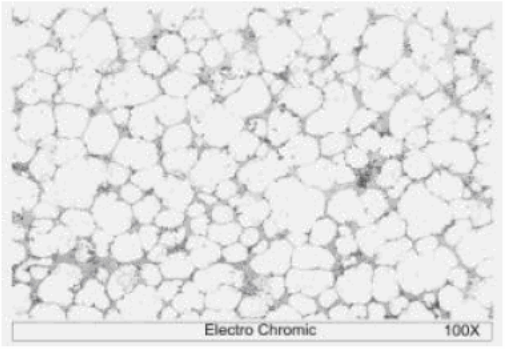

Figure 7: Traditional type wide gap joint on an X-45 substrate.

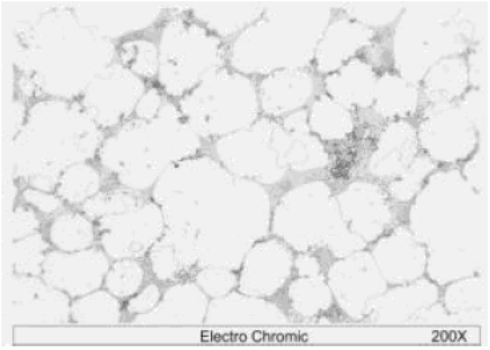

Figure 8: Traditional type wide gap joint on on an X-45 substrate.

Element	Phase A	Phase B	Phase C
Cr (at.%)	8.30	5.97	40.55
Co (at.%)	4.52	7.67	40.28
Ni (at.%)	0.91	1.66	9.02
Zr (at.%)	8.76	13.14	0.13
Ta (at.%)	68.70	67.04	0.23
W (at.%)	8.81	4.52	9.79

Table 10. Semi-quantitative analysis of the phases present in the traditional type wide gap braze

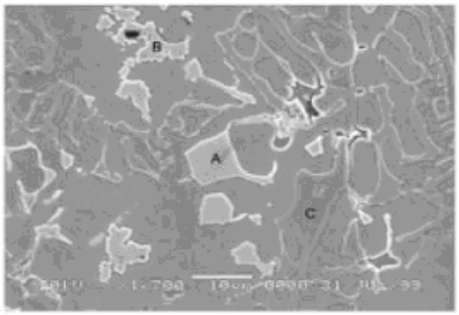

Figure 9: Location where the phases were identified.

Alternative Type Wide Gap Brazed Joints

Figures 10 and 11 shows the microstructure of the alternative type wide gap brazed joint on X-45 base metal. The wide gap brazed area is a finer grained structure (as seen in Figures 10 and 11) when comparing with Figures 7 and 8. The boride phases are discrete phases as seen in figure 11, and are not a network of elongated brittle boride phases as compared with those in Figure 8. The absence of the network of brittle boride phases in the wide gap joint, is the predominant reason for the increase in mechanical properties, including elongation. Figure 12 shows an area in the wide gap brazed joint, along the grain boundary, where 2 phases were analysed. The 2 phases identified were probably a W-Cr rich boride phase and a Cr carbide phase as seen in Table11. (The EDAX system on the SEM could not detect the elements C and B).

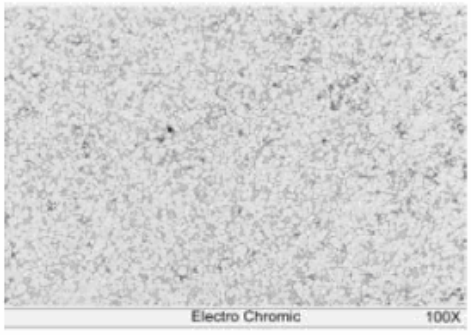

Figure 10: Alternative type wide gap joint on an X-45 substrate.

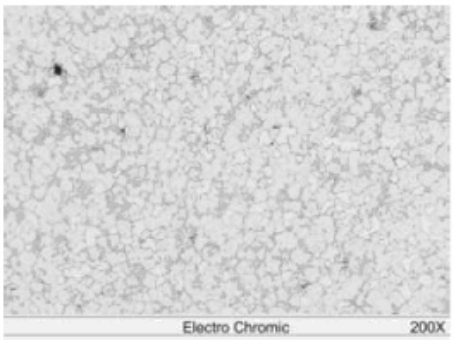

Figure 11: Alternative type wide gap joint on an X-45 substrate.

Element	Phase A	Phase B
Cr (at.%)	19.18	77.04
Co (at.%)	42.94	19.21
Ni (at.%)	3.93	1.11
Zr (at.%)	0.46	0
Ta (at.%)	4.46	0
W (at.%)	29.04	2.64

Table 11. Semi-quantitative analysis of the phases present in the alternative type wide gap braze

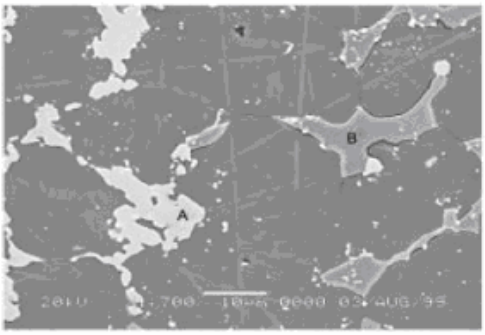

Figure 12: Location where the phases were identified.

PROCESS DEMONSTRATION

Figures 13 and 14 show the brazed repaired cracked areas, which were routed out in Figures 1 and 3. Figure 15 shows the brazed built up hook-fit region previously shown in Figure 4.

Figure 13: Brazed repaired region.

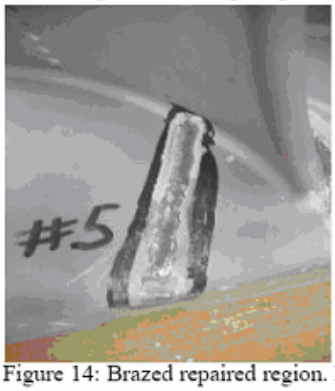

Figure 14: Brazed repaired region.

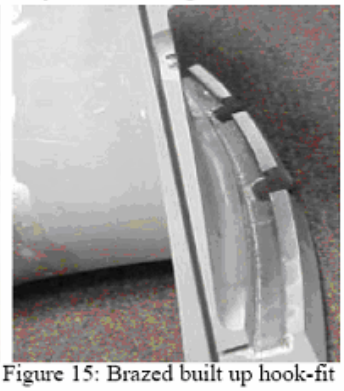

Figure 15: Brazed built up hook-fit

SUMMARY AND CONCLUSIONS

- The use of the alternative wide gap braze process, results in a repaired joint, which has mechanical properties (tensile and stress rupture) equivalent to that of the base metal.
- The microstructure of the joint shows no signs of large networks of brittle boride phases, known to significantly reduce mechanical properties and ductility. Only isolated boride phases were seen in the repaired area.
- The alternative wide gap braze process yields superior mechanical properties when comparing with the traditional wide gap brazing process.
- Based on the metallurgical and mechanical results obtained in this research project, the use of the alternative wide gap braze process is a suitable alternative to the Gas Tungsten Arc (GTA) weld approved repair process specified by the original engine manufacturer (OEM).
- The alternative process is ideally suited for crack repair, wall thickness repair of the convex and concave surfaces and dimensional restoration of the hook fit and race track areas of all Co-based vanes.
- This alternative process also works well on Ni-base superalloy components and this will form the basis of a paper in the near future.

REFERENCES

1. Demo, W.A and Ferrigno, S.J, 1992, "Brazing method helps repair aircraft gas – turbine nozzles", Advanced Materials and Processes, Vol 141, No.3, pp43-45
2. Wustman, R.D and Smith, J.S, 1996, "High strength diffusion braze repairs for gas turbine components", ASME paper 96-GT-427
3. Bell, S, 1985, "Repair and Rejuvenation procedures for aero gas-turbine hot section components", Material Science and Technology, Aug, Vol 1, pp629
4. Ellison, K.A, Lowden, P and Liburdi, J, 1992, "Powder metallurgy Repair of Turbine Components", ASME paper 92-GT-312
5. Metals Handbook, Vol 3, 9th edition, pp. 258 and 268, ASM International

APPENDIX D

MIGLIETTI, W.M.A. "WIDE GAP DIFFUSION BRAZE REPAIR OF NI-BASED INDUSTRIAL TURBINE VANES". PROCEEDINGS OF THE 6^{TH} *INTERNATIONAL CONFERENCE ON BRAZING, HIGH TEMPERATURE BRAZING AND DIFFUSION WELDING*. DVS BERICHTE, NO. 212. 8-10 MAY 2001. AACHEN, GERMANY. PP. 107-112.

WIDE GAP DIFFUSION BRAZE REPAIR OF Ni-BASED INDUSTRIAL TURBINE VANES

W.M.A. Miglietti - Sermatech International, Inc.

ABSTRACT

During the industrial turbine engine operation, cracks develop on the vanes as a result of thermal fatigue. Other damage found includes pitting and dents resulting from corrosion/oxidation and FOD (foreign object damage) respectively. Erosion damage is also commonly found on the airfoils. This paper describes the vacuum wide gap diffusion brazing repair process used to repair all of the above-mentioned damage, including braze build up. As a means of qualifying the high temperature diffusion braze process, both metallurgical and mechanical property evaluations were carried out. The metallurgical evaluation consisted of optical and scanning electron microscopy. The wide gap diffusion brazed area consisted of a fine-grained structure with carbide and intermetallic phases dispersed both intergranularly and intragranularly. The mechanical evaluations undertaken were tensile tests, stress rupture tests and low and high cycle fatigue tests. These results were equivalent to mechanical properties of the IN738, IN939, and Rene 80 Ni-based superalloys, which are the base metals that many of the vanes are cast from.

1. INTRODUCTION

Narrow gap brazing has been utilised for decades now to repair aircraft engine vane and nozzle segments. It has only being the last 5 years that wide gap brazing has been utilised for Industrial Gas Turbine (IGT) vane and nozzle repairs. The wide gap brazing process was made popular by GE's and Pratt and Whitney's ADH (activated diffusion healing) [1] and Turbofix processes respectively. Many repair vendors have their own proprietary wide gap braze process such as SNECMA's RBD (rechargement per brasage diffusion), Howmet's ESR (effective structural repair) [2] and Chromalloy's SRB (surface reaction braze) [3]. Other wide gap joining processes available are LPDS (liquid phase diffusion sintering), Liburdi's LPM (Liburdi powder metallurgy) [4] and Sermatech's "SermaFill" process [5]. The objective of this paper is to describe the use of an alternative wide gap braze process for IGT vane repairs, and to compare this process with the traditional wide gap braze process. A traditional wide gap process is referred to as, when a mixture/blend of superalloy powder and braze powder is utilised. The mixtures are usually a 40/60, 50/50 or a 60/40 blend by weight. The alternative wide gap process is proprietary and hence exact precise temperatures and times, chemical compositions etc. cannot be documented; nevertheless, ranges of temperature and times are documented. This process was qualified by undertaking a metallurgical evaluation and a mechanical property evaluation to show that metallurgically sound and high strength joints resulted. This alternative process was used to restore wall thickness on the concave and convex surfaces of the airfoil, and repair cracks, pits and dents.

Many of the IGT vanes are manufactured from Ni-based alloys like IN738, IN939 and Rene80. The chemical composition of the materials is given in **Table 1.** The high volume fraction of gamma prime (γ'), a Ni_3Al phase, enables these alloys to possess remarkable mechanical properties at elevated temperatures. **Figures 1 and 2** show typical examples of "craze" cracking and leading and trailing edge cracking on an IN738, Siemens V84.2, Row 2 vane and an Alstom, Tornado, CT2, stator segement, respectively. The largest width of crack found on these engine sets was 1.5mm. As a result of these large gaps, conventional narrow gap brazing cannot be utilised as a repair technique. For the crack repair, paste is used as the medium for the repair; whereas, for concave and convex dimensional build up, tape is utilised. The largest width of cracks found on these engine sets was 1.5mm. Therefore for the process qualification, the mechanical property tests

Table 1: Base Metals (BM) Composition, Wt. %

Alloy	C	Co	Cr	Ni	Mo	Al	W	Ta	Nb	Ti	Zr
IN738	0.17	8.5	16	Bal	1.7	3.4	2.6	1.7	0.9	3.4	0.1
IN939	0.15	19	22.5	Bal	0	1.9	2.0	1.4	0	3.7	0.1
Rene80	0.17	9.5	14	Bal	4	3	4	0	0	5	0.1

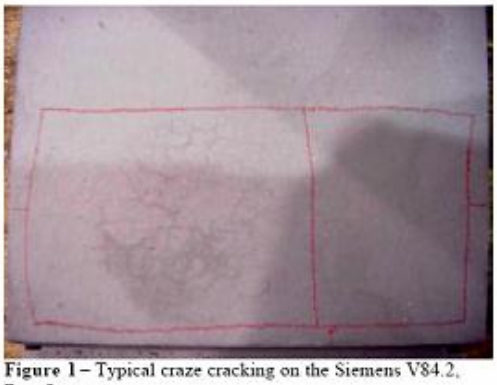

Figure 1 – Typical craze cracking on the Siemens V84.2, Row 2 vane.

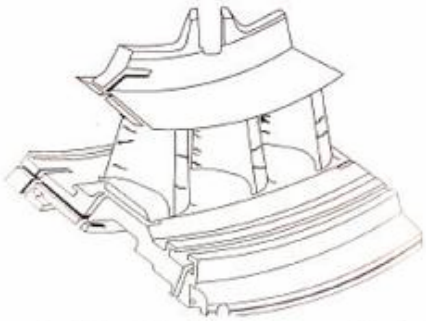

Figure 2 – Typical view from the concave side, showing leading edge, trailing edge and shroud/buttress cracking on the Alstom Tornado 2nd stage stator segment.

(namely tensile, stress rupture and fatigue) where undertaken on samples where the joint gap was 1.5mm. The process is not limited to this gap and the largest gap repaired to date has been 10mm.

2. EXPERMENTAL PROCEDURE

Tensile tests at room temperature (21°C) and elevated temperatures, as well as stress rupture and low and high cycle fatigue tests were undertaken. The test specimens were prepared in a butt joint configuration as seen in **fig 3**. The joint is in the centre of the gauge length and was 1.5mm wide.

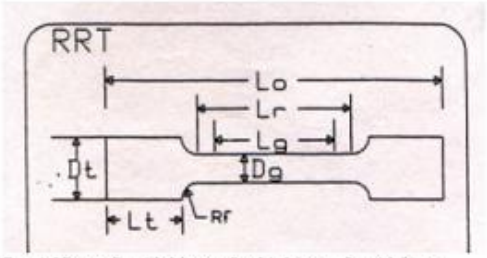

D_g=4.57mm, L_g=18.29mm, L_r=21.84mm, L_o=46.51mm, R_f=3.18mm, D_t=(5/16-24NF-2A inches) and L_t=9.53mm

Figure 3 – Configuration for the mechanical test specimens.

3. MECHANICAL TEST SPECIMEN PREPA RATION

Mechanical test specimens according to the configuration shown in **fig 3** were prepared as follows:

a) Obtain investment cast IN738, IN939 and Rene80 material.
b) Machine rectangular sections of 12.5mm X 12.5mm X 55.9mm.
c) Cut sample in half.
d) Grind the mat ing surfaces flat.
e) Grit blast surfaces with silicon carbide.
f) Shim gap at 1.5mm .
g) Apply paste to the joint gap.
h) Place samples in fixture to maintain alignment.
i) Set in vacuum furnace.
j) Process between 1120°C and 1200°C.
k) Isothermally process for 4-20 hours.
l) Age at 843°C/ 24 hours for IN738 or age at 900°C/ 24 hours + 700°C/16 hours for IN939, or age at 1050°C/ 4 hours + 845°C/16 hours for Rene80.
m) Machine samples to the configuration shown in **fig 3**.
n) Send the machined specimens for X-ray analysis to determine if porosity greater than 0.5mm exists and for lack of bonding to the mating surfaces.

4. RESULTS AND DISCUSSION OF MECHANICAL PROPERTY TESTING

Table 2 below shows the results of the tensile tests undertaken at room temperature and elevated temperatures of 650°C, 760°C and 982°C on the alternative wide gap brazed joints for IN738. As can be seen the tensile and yield strengths are equivalent to the values quoted in the Metals Handbook. The elongation of the alternative type wide gap brazed joints appears low, when compared to the values quoted in the Metals Handbook. There is a good explanation for this, which will be discussed later. Nevertheless the RA values are equivalent to the base metals values and hence the joints possess reasonable ductility.

Table 2: Tensile Strength of IN738 processedwith "SermaFill"5 Filler Metal

TEMPERA - TURE		TENSILE STRENGTH		YIELD STRENGTH		ELONG ATION	RA
°C	°F	MPa	ksi	MPa	ksi	%	%
21	70	1011	146.5	882	127.8	3.1	4.7
21	70	886	128.4	866	125.5	1.4	3.6
21	**70**	**1050**	**152**	**865**	**125.4**	**5**	**5**
650	1200	827	120	671	97.3	6.0	5.6
650	1200	765	111	661	95.8	3.3	4.0
650	1200	753	109	682	98.9	4.1	3.7
650	**1200**	**850**	**123**	**655**	**95**	**5**	**5**
760	1400	908	131.6	747	108.3	3.9	5.9
760	1400	944	136.8	768	111.3	3.8	5.6
760	**1400**	**965**	**140**	**795**	**115**	**6**	**?**
982	1800	412	59.7	319	46.2	2.0	8.2
982	1800	372	53.9	317	45.9	1.6	6.1
982	**1800**	**435**	**63**	**325**	**47.1**	**6.5**	**?**

NOTE Values in Bold are for IN738 parent alloy (Metals Handbook Vol3, ninth edition)

To verify if the elongation is as low as the data indicates, some IN738 material was taken from the root area of a W501F, 1st stage blade. This material was machined to the configuration shown in **fig 3**.

Table 3 shows the results of the IN738 specimens removed from the blade root. As seen in **Table 3** the mechanical properties of the IN738 taken from the actual blade casting is lower than that quoted in the Metals Handbook, including the ductility. Therefore the alternative wide gap brazed joints have ductility in the order of 80% of the IN738 casting material. This is acceptable and the 20% loss in ductility is attributed to the few brittle intermetallic phases present in the 1.5mm wide gap joint.

Table 3: Tensile strength of IN738 material taken from the root of a blade.

TEMPERA - TURE		TENSILE STRENGTH		YIELD STRENGTH		ELONG ATION	RA
°C	°F	MPa	ksi	MPa	ksi	%	%
21	70	828	120	759	110	3	3
21	**70**	**1050**	**152**	**865**	**125.4**	**5**	**5**

NOTE Values in Bold are for IN738 parent alloy (Metals Handbook Vol3, ninth edition)

Table 4, shows the stress rupture properties of the alternative type wide gap joints for IN738. As seen in **Table 4**, the stress rupture properties of the joints are a minimum of 89% of the base metals stress rupture properties.

To compare the results of the alternative type wide gap joints with a more traditional wide gap braze process, a 50% IN738 and 50% BRB braze (Ni-13.5Cr-7.5Co-4Al-2.5B) mixture was developed. Some samples were brazed with the same joint gap and at the same process parameters as those of the alternative type wide gap brazed joints.

Tables 5 and 6 show the tensile test results and stress rupture results respectively, of the joints brazed with the 50/50 mixture. As seen in these tables, the strength of the brazed joint is 40%–53% of the base metals strength, the elongation is 33%--50% of the cast IN738 blade material

Table 4: Stress rupture properties of IN738 processed with "Sermafill" 5 Filler Metal

TEMPERATURE		STRESS	HOURS TO FAILURE	ELONGATION	RA
°C	°F	MPa	hrs	%	%
843	1550	345	190.3	1.7	?
843	1550	345	93.7	1.9	?
843	1550	345	89	2.3	?
843	1550	345	97.3	1.8	?
843	**1550**	**345**	**100**	**5**	**5**
829	1525	345	203.37	4.4	?
829	**1525**	**345**	**223.02**	**6.7**	**?**
982	1800	124.2	453.2*	5.5	?
982	**1800**	**124.2**	**807.2**	**5.2**	**?**

NOTE: Values in Bold are for IN738 material, taken from the root of a blade

* means that failure occurred in the base metal

and the stress rupture life varies from 7.4-11.9% of the parent metals life. This is undesirable if the objective is to have a structural repair, where the properties of the repaired areas are equivalent to the base metal. Clearly the alternative wide gap type joints have superior mechanical properties when compared to a more traditional type wide gap braze joint, and the properties are equivalent to the base metal as seen in **Tables 2 and 4.**

Table 5: Tensile strength of IN738 brazed with a traditional type filler metal (50%IN738 + 50%BRB)

TEMPERATURE		TENSILE STRENGTH		YIELD STRENGTH		ELONGATION	RA
°C	°F	MPa	ksi	MPa	ksi	%	%
21	70	527	76.4	527	76.4	1.4	2.4
21	70	502	72.8	502	72.8	1.8	2.2
21	70	559	81	559	81	1.0	2.9
21	**70**	**1050**	**152**	**865**	**125.4**	**5**	**5**
650	1200	322	46.7	322	46.7	2.5	1.6
650	1200	441	63.9	441	63.9	1.2	1.9
650	1200	338	49	338	49	1.9	5.2
650	**1200**	**850**	**123**	**655**	**95**	**5**	**5**

NOTE: Values in Bold are for IN738 Alloy (Metals Handbook, Vol. 3, ninth edition)

Table 6: Stress Rupture properties of IN738 brazed with a traditional type filler metal (50%IN738 + 50%BRB)

TEMPERATURE		STRESS LEVEL		HRS TO FAILURE	ELONGATION	RA
°C	°F	MPa	ksi	hrs	%	%
843	1550	345	50	11.9	?	?
843	1550	345	50	7.4	?	?
843	**1550**	**345**	**50**	**100**	**5**	**5**

NOTE: Values in Bold are for X-45 alloy (Metals Handbook, Vol3, ninth edition)

Table 7 shows the results of the tensile tests undertaken at room temperature and elevated temperature of 650°C, on the alternative type joints for IN939. As can be seen the tensile and yield strengths are equivalent to the values of the cast material. The elongation of the joints is 50-73% of the base metals values. This is attributed to the intermetallic phases present in the joint. The RA values are however equivalent to that of the base metal, hence the joints do possess reasonable ductility. As seen in **fig 4** the stress rupture properties of the joints are a minimum of 90% of the base metals.

Table 7: Tensile Strength of IN939 processed with "SermaFill"3 Filler Metal

TEMPERATURE		TENSILE STRENGTH		YIELD STRENGTH		ELONGATION	RA
°C	°F	MPa	ksi	MPa	ksi	%	%
21	70	920	133.3	670	97.1	2.2	3.6
21	70	859	124.5	696	100.9	1.8	4.3
21	70	817	118.4	750	108.7	1.7	7.7
21	70	999	144.8	651	94.3	1.5	3.0
21	**70**	**897**	**130**	**690**	**100**	**3**	**5.0**
650	1200	768	111.3	625	90.6	1.5	4.0
650	1200	860	124.7	654	94.8	2.1	5.1
650	**1200**	**863**	**125.1**	**621**	**90**	**3**	**5.0**

NOTE: Values in bold are for cast IN939 material taken from a shroud buttress section.

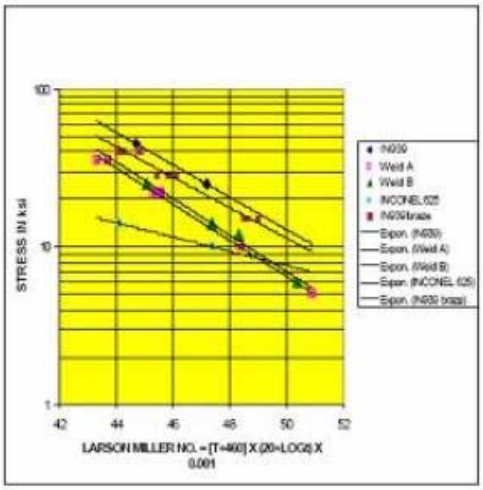

Figure 4 – Larson Miller Plot of the stress rupture properties of the alternative type wide gap joints versus a number of weld filler metals.

In fact **fig 4,** also shows that the alternative wide gap brazed joints have superior stress rupture lives when compared to 3 different weld filler metals viz. IN625, Weld A and Weld B. IN625 is well utilised as a filler metal for non-structural repair applications, because of its good ductility and ease of welding. However as can be seen, this filler metal has poor stress rupture life when compared to IN939. Two proprietary higher strength weld filler metals based on the elements Ni-Cr-Co-Mo-W-Ti-Al-C were developed as substitutes for IN625, and even these filler metals, did not even have the stress rupture properties equivalent to those of the LPDB joints. It should be realised that IN939, as a result of its high total Al + Ti content is not readily weldable and suffers from strain age cracking.

A similar trend of the results for the alternative wide gap brazed joints of IN738 and IN939 was obtained for Rene80. As seen in **Tables 8, 9 and 10** , the mechanical properties of the wide gap brazed joints are equivalent to that of the base metal.

Table 8 Tensile properties at 25°C of Rene80 and Rene80 alternative wide gap brazed joints.

Property	80 Sermafill	Rene80*
Tensile (MPa)	892.9	870.1
Yield (MPa)	857.7	700.4
Elongation (%)	0.6	1.8
RA (%)	1.5	3.5

- *specimens were in the solution and aged condition and not in the Hipped, solution and aged condition

Table 9: Tensile properties at 871°C of Rene80 and Rene80 altemative wide gap brazed joints.

Property	80 SermaFill	Rene 80*
Tensile (MPa)	103.2	91.9
Yield (MPa)	86.6	63.2
Elongation (%)	1.9	6.6
RA (%)	1.2	8.1

- *specimens were in the solution and aged condition and not in the Hipped, solution and age d condition

Table 10: Stress rupture properties of Rene80 and Rene80 wide gap braze.

Alloy	Cond-ition	Test temp	Stress (MPa)	Hrs	Elong %	RA %
80 Serma fill	Brazed + Solution + aged	871°C	345	22.6	4.9	6.4
		871°C	311	59	3.9	7.7
		871°C	276	124	3.0	11.3
		927°C	242	26.1	3.7	7.4
Rene 80* base metal	Solution + aged	871°C	345	18.1	?	?
		871°C	311	44	10.2	18.4
		871°C	276	122.6	?	?
		927°C	242	31.5	?	?

- *specimens were in the solution and aged condition and not in the Hipped, solution and aged condition

In summary the tensile and stress rupture data of the alternative wide gap brazed joints for IN738, IN939 and Rene80 are equivalent to that of the base metal.

Figure 5 shows the stress controlled, high cycle fatigue results generated at 760°C on IN738 base metal, which were undertaken at a frequency of 10Hz, with the minimum stress (σ_{min}=0); therefore maximum stress = total stress (σ_{max} = σ_{total}). As can be seen in fig 5, the endurance limit defined as the stress corresponding to 10^7 cycles is 345MPa (50ksi), even though at 414MPa (60ksi) the samples at 5000000 cycles had not failed.

Figure 6 shows the strain controlled low cycle fatigue results generated at 870°C on IN738 base metal, which were undertaken at a constant strain rate of 0.01 S^{-1}, with a symmetrical triangular wave form. The LCF tests were conducted between total strain values of 0.5% and 1.5%, and a corresponding test frequency ranging between 1Hz and 0.33Hz. At strain levels of 0.6% and higher the LCF life is 50%--75% of the base metals life. At strain levels less than 0.6%, the LCF life is equivalent to that of the base metal.

In summary the high cycle fatigue properties, i.e. the endurance limit corresponding to 10^7 cycles, of the alternative wide gap brazed joints is equivalent to that of the base metal. At strain levels of less than 0.6%, the low cycle fatigue life is equivalent to that of the base metal.

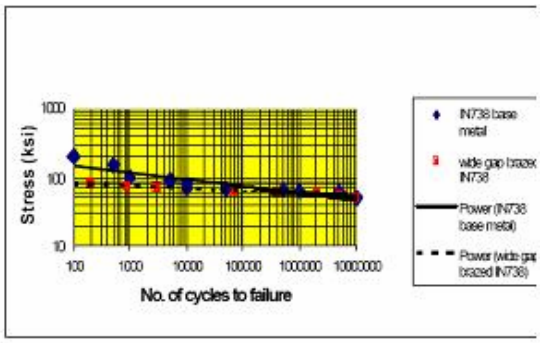

Figure 5 - High cycle fatigue properties at 760°C of IN738 and the alternative wide gap brazed IN738.

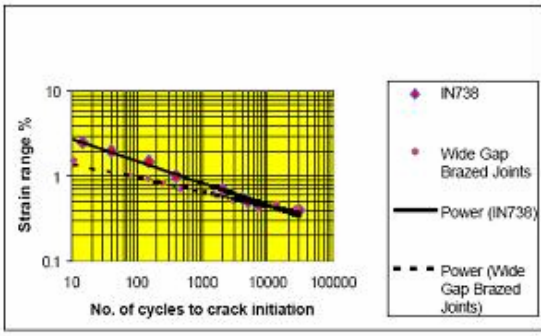

Figure 6 - LCF properties at 870°C of IN738 and the alternative wide gap diffusion brazed IN738.

5. METALLURGICAL RESULTS AND DISCUSSION

Figure 7 shows the macrograph of a cross section taken through the alternative type wide gap braze repair of the IN738, V84.2, row 2 vane. As can be seen the "craze-cracked" area was machined away and this area was filled with the alternative wide gap braze filler metal

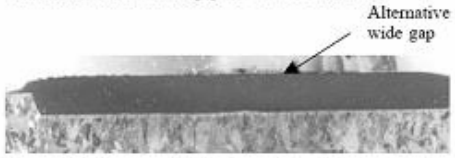

Figure 7 – Macrograph taken through the alternative wide gap braze repaired area of the V84.2, row 2 vane. Mag. 5X

Figure 8 shows the excellent bonding/ adhesion to the IN738 vane material. A fine-grained microstructure is evident. Some minor microporosity can be seen in the micrograph, but this microporosity level is acceptable. **Figure 9** shows the fine grained structure of the alternative type wide gap brazed joint, with intermetallic phases dispersed intergranularly.

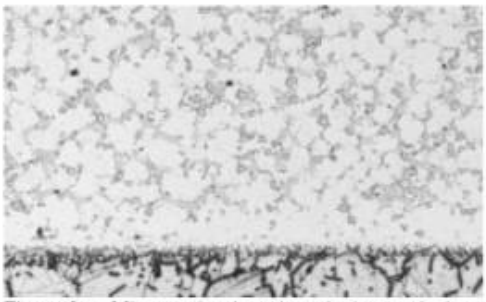

Figure 8 – Micrograph taken through the repaired area showing excellent bonding to the vane material. Mag. 75X

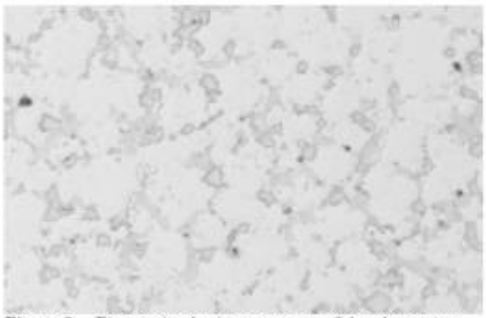

Figure 9 – Fine grained microstructure of the alternative wide gap brazed joint with intermetallic phases dispersed intergranularly. Mag. 150X

Figure 10 shows the macrograph of a cross section taken through the alternative wide gap braze repair of the IN939, Tornado 2nd stage stator segment. As can be seen the filler metal has flowed completely down to the bottom of the crack and has bonded excellently to the sidewalls of the routed out crack. Also the microporosity is less in the joint, when compared to that of the base metal.

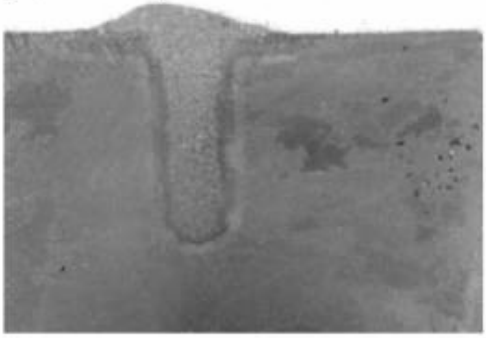

Figure 10 – Macrograph of the joint taken through the alternative wide gap braze repair of the Tornado, 2nd stage stator segment. Mag. 5X

Figure 11 shows a cross section taken through a "through" crack at the trailing edge of the airfoil. Once again there is good bonding to the sidewalls of the routed out crack.

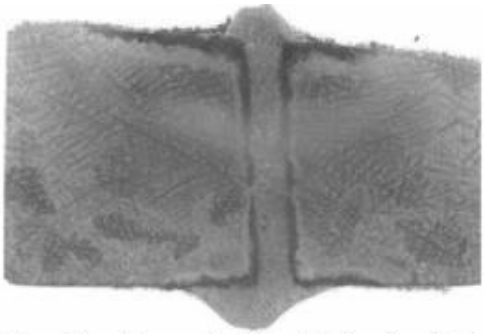

Figure 11 – Macrograph of the joint taken through the alternative wide gap braze repaired area of the Tornado, 2nd stage stator segment. Mag 5X

Figure 12 shows the micrograph of the repaired area. It consists of a fine-grained structure and there is good bonding/adhesion to the sidewalls. **Figure 13** shows the joint to consist of equiaxed grains with intermetallic phases dispersed intergranularly.

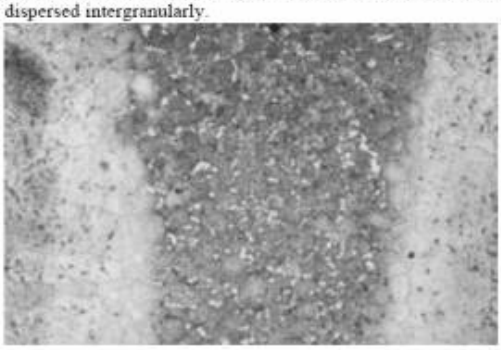

Figure 12 - Micrograph taken through the repaired area showing a fine-grained microstructure. Mag. 45X

The traditional wide gap brazed samples used to produce the mechanical test results shown in **Tables 5 and 6**, were also analysed. As a reminder a filler metal of 50% IN738 powder and 50%BRB braze was utilised. As seen in **fig 14** the joint in the stress rupture sample consist of a mixture of fine and coarse grains with a continuous layer of intergranular intermetallic phases. This is in contrast to the discrete isolated and discontinuous intermetallic phases that were present in the joints seen in **fig's 12-13. Figure 15** shows the continuous intergranular intermetallic phases present in the joint. The bright "blocky and dark grey intermetallic phases can be clearly seen along the grain boundaries.

6. FIRST ARTICLE REPAIR DEMONSTRATION

Figure 16 shows areas on the V84.2, row 2 vanes, which were routed out and processed with the alternative wide gap filler metal, plus subsequent heat treatment **Figure 17** shows the Tornado, 2nd stage stator segment after complete repair including heat treatment and Sermaloy J coating. (Sermaloy J is an aluminide coating that is proprietary to Sermatech International, Inc.)

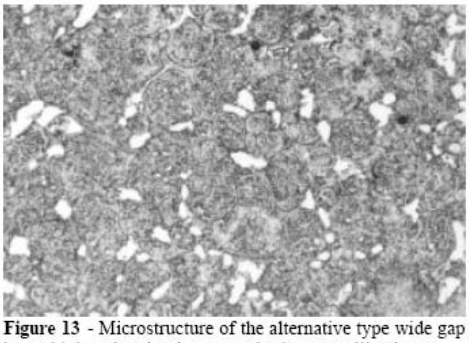

Figure 13 - Microstructure of the alternative type wide gap brazed joint, showing intergranular intermetallic phases. Mag. 150X

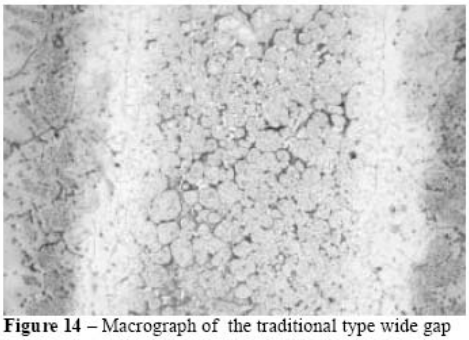

Figure 14 – Macrograph of the traditional type wide gap brazed joint taken from a stress rupture sample. Mag. 45X

7. CONCLUSIONS

The use of the alternative wide gap braze process, results in a repaired joint, which has mechanical properties (tensile, stress rupture and fatigue) equivalent to that of the base metal. These properties are far superior to those of traditional and conventional wide gap braze processes.

The microstructure of the joint shows no signs of large networks of brittle boride phases, known to significantly reduce mechanical properties and ductility. Only isolated and discrete intermetallic phases were seen in the repaired area.

Based on the metallurgical and mechanical results obtained in this research project, the use of the alternative wide gap braze process (which Sermatech International, Inc. has as there trademark "SermaFill") is a suitable alternative to the traditional Gas Tungsten Arc weld approved repair process.

This alternative wide gap braze process ("SermaFill") is ideally suited for crack repair, including "craze cracking", wall thickness repair of the convex and concave surfaces and dimensional restoration of Ni and Co-based IGT vanes.

8. REFERENCES

[1] Demo, W.A. and Ferrigno, S.J., 1992, "Brazing method helps repair aircraft gas –turbine nozzles", Advanced Materials and Processes, Vol. 141, No.3, pp43-45.

[2] Wustman, R.D. and Smith, J.S., 1996, "High strength diffusion braze repairs for gas turbine components", ASME paper 96-GT-427.

[3] Bell, S., 1985, "Repair and Rejuvenation procedures for aero gas-turbine hot section components", Material Science and Technology, Aug, Vol. 1, pp629

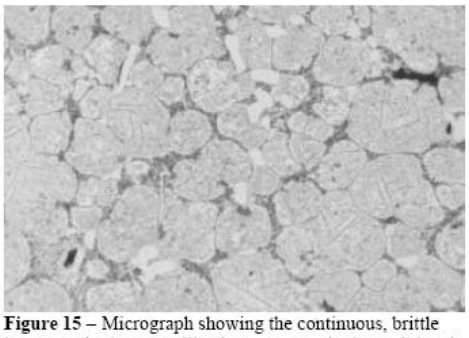

Figure 15 – Micrograph showing the continuous, brittle intergranular intermetallic phases present in the traditional type wide gap brazed joints. Mag. 150X

Figure 16 – V84.2, row 2 vanes repaired with the alternative wide gap braze process.

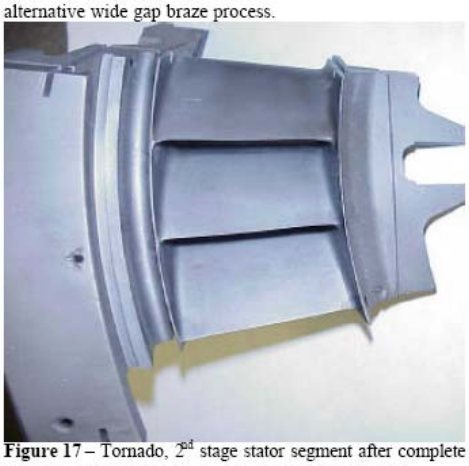

Figure 17 – Tornado, 2nd stage stator segment after complete repair including heat treatment and Sermaloy J coating.